

PHYSICAL AND THEORETICAL STUDIES OF  
LOCALIZED ORGANIC BIRADICALS

Thesis by  
Aaron Henry Goldberg

In Partial Fulfillment of the  
Requirements for the Degree of  
Master of Science

California Institute of Technology  
Pasadena, California

1982/3

(submitted August 20, 1982)

**ACKNOWLEDGEMENTS**

When I first announced my decision to leave Caltech (to pursue a degree in law), one person responded, "'Boy, you must have really hated it around this place'". Initially, I was surprised by the comment, but it gradually occurred to me that other people were probably coming to the same conclusion. At last I have a chance to set the record straight. Don't worry — I'm not going to say that the last two years have been the best of my life. I've never been a convincing liar (even on paper) and besides, it's doubtful that anyone reading this would be stupid enough to believe me. Still, the truth is that the past two years have been two very good ones, and to a large extent, I have the people at Caltech to thank for that.

First and foremost I must thank my advisor, Dennis Dougherty. Working for him has been both enjoyable and rewarding — in fact, perhaps too much so. It made an already difficult decision to leave even harder. I am also extremely grateful to the other members of the Dougherty group. Much of my work was performed in collaboration with Lisa McElwee-White and Moon Ho Chang, and those portions which were not, were aided by them nonetheless.

Many thanks are due to Peter Dervan and the entire Dervan group. As the only other physical organic group at Caltech, they have served as an extended family of sorts. They have been a constant source of advice, support, GC columns, and softball tips.

I am further indebted to Bill Goddard and his students — particularly John Low and Art Voter. Without their help, half of my work would simply not have been possible. I also acknowledge Craig

Martin for his frequent help with the ESR spectrometer. Finally, I wish to express my deep appreciation to Jan Owen for typing this manuscript so many times as it developed from draft to paper to candidacy report and finally to Master's Thesis.

## ABSTRACTS

## Section I. Introduction

Section II. Singlet-triplet energy gaps in localized 1,3-biradicals have been investigated using ab initio electronic structure theory. Analysis of both the molecular orbital and generalized valence bond wavefunctions allows one to follow the complex interplay between through-bond and through-space interactions. When the two effects are of similar magnitude, a triplet ground state is possible. However, when one significantly dominates the other, a singlet ground state is expected. Extension of the analysis to other systems and the implications of the results for experimental studies of localized biradicals are discussed.

Section III. Several unsuccessful attempts to observe the triplet cyclobutane- and cyclohexane-1,3-diyls through low temperature photolysis of the corresponding azo and azoxy compounds are reported. The reasons for these failures are considered together with their implications for the observation of other localized biradicals.

Section IV. Photolysis of either 7-(2,3-diazabicyclo[2.2.1]hept-2-ene) spirocyclopropane or 7-(2,3-diazabicyclo[2.2.1]hept-2-ene) spiro-5'-bicyclo[2.1.0]pentane in a glassy matrix at 8°K leads to observation of a triplet ESR spectrum. Both signals exhibit zero-field splitting parameters which are typical of delocalized systems ( $|D/hc| = 0.0255$  and  $|E/hc| = 0.003$

$\text{cm}^{-1}$ ). In addition, they are stable at temperatures well in excess of  $85^\circ\text{K}$ . Several possible sources of the two spectra are discussed.

Section V. A program for the ab initio calculation of zero-field splitting parameters in localized biradicals is developed. The results for several 1,3-biradicals are presented.

## TABLE OF CONTENTS

## SECTION I. INTRODUCTION

SECTION II. EFFECTS OF THROUGH-BOND AND THROUGH-SPACE  
INTERACTIONS ON SINGLET-TRIPLET ENERGY GAPS  
IN LOCALIZED BIRADICALS

Abstract.....	4
Introduction.....	5
Computational Methods.....	7
Results and Discussion.....	8
Through-space Interactions.....	10
Through-bond Interactions in	
(0,0)-Trimethylene.....	15
Trimethylene Derivatives.....	23
Other Systems.....	25
Conclusion.....	29
References and Notes.....	31

SECTION III.    ATTEMPTED OBSERVATION OF THE CYCLOBUTANE-  
AND CYCLOHEXANE-1,3-DIYLS

Introduction.....	36
Results and Discussion.....	37
2,3-Diazabicyclo[2.1.1]hex-2-ene.....	37
2,3-Diazabicyclo[2.1.1]hex-2-ene N-oxide...	38
2,3-Diazabicyclo[3.2.1]oct-2-ene.....	39
Conclusion.....	40
Experimental.....	40
References and Notes.....	43

SECTION IV.    ESR STUDIES OF SPIROPENTANE-BASED  
REARRANGEMENTS

Introduction.....	44
Results and Discussion.....	48
Conclusion.....	56
Experimental.....	56
References and Notes.....	58

SECTION V.      DEVELOPMENT OF A COMPUTER PROGRAM FOR  
CALCULATING ZERO-FIELD SPLITTING PARAMETERS IN  
LOCALIZED BIRADICALS

Introduction.....	62
Overview of Various Possible Approaches.....	63
The Numerical Integration Method.....	65
Programming Considerations.....	68
Results and Discussion.....	69
References and Notes.....	72
Appendix A. Description of Input Data for Zero-field Splitting Programs.....	75
Appendix B. Sample Input Deck.....	79
Appendix C. ZFS2: A Program for Calculating Zero-field Splitting Parameters in Systems Without Symmetry.....	83
Appendix D. ZFS3: A Program for Calculating Zero-field Splitting Parameters in Systems With $C_{2v}$ Symmetry.....	91

## **Section I**

### **Introduction**

## I. Introduction

Localized biradicals,<sup>1</sup> unlike their more stable counterparts, delocalized biradicals, are usually not isolated or detected by spectroscopic methods but rather are assumed intermediates on the basis of a substantial body of chemical evidence.<sup>2</sup> ESR observation of the first such species, cyclopentadiyl (1), was reported by Closs in 1975.<sup>3</sup> Closs' result promised to remove simple localized biradicals from the realm of "'permissible intermediate'" and "'theoretical model'" to that of thermodynamically and kinetically characterized reactive intermediate. Unfortunately, extension of the experiment to other fundamental localized biradical systems has thus far not proved possible.



1

In the current work the reason for this failure is elucidated. First it is shown that only a small number of localized biradicals should exhibit a triplet ground state — an important requirement for ESR observation of such species (Section II). It is then demonstrated that only a small fraction of even these few biradicals will be observable under the conditions of the Closs experiment. In several instances, the precursor molecules lack the proper photochemistry, while in others, the biradicals may be too flexible to permit an extended lifetime (Section III).

Even though it seems unlikely that many other localized biradicals will ever be observed by ESR, studies on the one fundamental system which can be observed in this manner may still provide useful information about such species. In Sections IV and V, two systems which are structurally similar to, but chemically quite different from 1 are investigated. This work takes advantage of both experimental and theoretical methods.

**References and Notes**

1. The term "'localized'" is used here in a classical sense, implying that the radical centers are not part of a conventional  $\pi$ -system. However, a major point of this work is that the radical centers do delocalize via the  $\text{CH}_2$  groups.
2. (a) Berson, J.A. In "'Rearrangements in Ground and Excited States, Vol. I'"; de Mayo, P., Ed.; Academic Press: New York, 1980; pp. 311-390. (b) Gajewski, J.J. "'Hydrocarbon Thermal Isomerizations'"; Academic Press: New York, 1981. (c) Wagner, P.J. In "'Rearrangements in Ground and Excited States, Vol. III'"; de Mayo, P., Ed.; Academic Press, New York, 1980; pp. 381-444.
3. Buchwalter, S.L.; Closs, G.L. J. Am. Chem. Soc. **1979**, 101, 4688-4694.

## Section II

### **Effects of Through-bond and Through-space Interactions on Singlet-Triplet Energy Gaps in Localized Biradicals**

**II. Effects of Through-bond and Through-space  
Interactions on Singlet-Triplet Energy Gaps  
in Localized Biradicals**

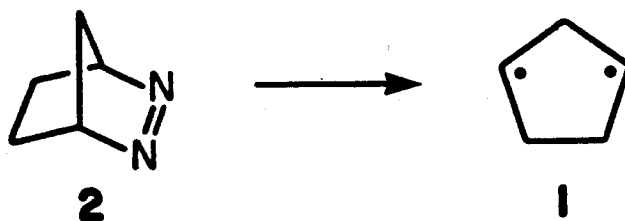
Aaron H. Goldberg and Dennis A. Dougherty\*

Contribution No. 6615 from the Crellin Laboratory of Chemistry,  
California Institute of Technology,  
Pasadena, California 91125

**Abstract:** Singlet-triplet energy gaps in localized 1,3-biradicals have been investigated using ab initio electronic structure theory. Analysis of both the molecular orbital and generalized valence bond wavefunctions allows one to follow the complex interplay between through-bond and through-space interactions. When the two effects are of similar magnitude, a triplet ground state is possible. However, when one significantly dominates the other, a singlet ground state is expected. Extension of the analysis to other systems and the implications of the results for experimental studies of localized biradicals are discussed.

## Introduction

Biradicals have long been postulated as intermediates in a variety of thermal and photochemical reactions.<sup>1</sup> More recently, direct observation of such species has become possible, and ESR studies of several highly delocalized biradicals have been reported over the last 15 years.<sup>2</sup> In 1975, Closs<sup>3</sup> photolyzed azoalkane **2** at 5.5°K and observed the ESR spectrum of the triplet state of 1,3-cyclopentadiyl (**1**). This landmark result promised to remove simple localized<sup>4</sup> biradicals from the realm of "permissible intermediate" and "theoretical model" to that of thermodynamically and kinetically characterized reactive intermediate. However, extension of the Closs experiment to other fundamental localized biradical systems has thus far not been possible. This failure is certainly not for want of effort,<sup>3,5,6</sup> and it suggests that insights into the factors which make the observation of **1** successful would be useful.<sup>7</sup>



Several lines of experimental evidence<sup>3</sup> and theoretical calculation,<sup>8</sup> indicate that **1** has a triplet ground state. It seems certain that this is a major factor which facilitates its direct observation by ESR. Direct observation of the singlet state of a localized biradical has not yet been accomplished, and in most cases

the lifetimes of such species must be quite short. If a biradical has a triplet ground state, however, the spin forbiddenness of the normal unimolecular decomposition pathways (e.g., ring closure) can increase the biradical lifetime. If the singlet-triplet energy gap is substantial, an additional enthalpic barrier to the  $T \rightarrow S$  conversion may also be operative. It is quite possible that a triplet ground state is a necessary criterion for ESR observation of certain types of nonconjugated biradicals. In the general case, however, one would not expect a triplet ground state for a localized biradical. Hund's rule does not apply to structures such as 1, since the atomic orbitals containing the unpaired electrons are not orthogonal.<sup>9</sup> Also, a weakly interacting pair of radicals does not generally exhibit a triplet ground state, as evidenced by the fact that  $S_0$  always remains below  $T_1$  in the homolytic dissociation of  $H_2$ .<sup>10</sup>

The present work was therefore undertaken to determine why 1 has a triplet ground state. While the ESR experiment on 1 provided the major impetus for this work, localized triplet biradicals have more recently been observed directly using laser flash photolysis techniques<sup>11</sup> and indirectly by CIDNP.<sup>12</sup> Clearly, knowledge of the factors which determine ground state spin multiplicity would be quite useful in designing and interpreting such experiments. This is especially so since singlet-triplet energy gaps greatly influence intersystem crossing rates, and thus significantly affect the lifetime and chemistry of biradicals and excited states in general.<sup>13</sup>

Our calculations reveal that the through-space interaction between the radical orbitals in 1 is surprisingly large, but it is almost exactly counteracted by an equally large through-bond effect.

Under such circumstances a triplet ground state can develop. In addition to quantifying the interactions in **1** and related molecules, we have analyzed the generalized valence bond (GVB) wavefunctions<sup>14</sup> for such structures. The GVB approach provides a simple, alternative model for the following interplay between through-bond and through-space interactions, and we have used it as a basis for the extension of our results for **1** to other systems.

### Computational Methods

All calculations were performed using a valence double-zeta basis set. For carbon, Dunning's contraction<sup>15</sup> (3s,2p) of Huzinaga's (9s,5p) basis set<sup>16</sup> was adopted, while for hydrogen a comparable (4s/2s) contraction was utilized,<sup>15</sup> with each Gaussian exponent scaled by a factor of 1.44.

Wave functions for triplet biradicals were obtained using Restricted Hartree-Fock (RHF) theory. However, an MCSCF procedure,<sup>17</sup> in which both the orbitals and their mixing coefficients were simultaneously optimized, was employed to yield a two-configuration wavefunction for each singlet. This level of theory has been shown to weight ionic and covalent terms properly,<sup>18</sup> and has been successfully employed in several recent studies of localized biradicals.<sup>8,19</sup> At this level, the triplet state of **1** lies 0.9 kcal/mol below the singlet.<sup>8</sup>

Our confidence in the reliability of this level of theory is further enhanced by the fact that more extensive CI calculations on **1** lead to only minor changes in the singlet-triplet gap. For example,

we have found that allowing all single and double excitations from the five  $\pi$ -orbitals (obtained separately for each state, as described above) into the  $\pi$  virtual space, increases the singlet-triplet gap to 1.15 kcal/mole.<sup>20</sup>

It should be emphasized from the start that quantitative prediction of singlet-triplet gaps is not the goal of the present work. We are principally interested in trends in the data and the underlying factors responsible for them. Even if the calculations are only semi-quantitatively accurate, we believe they should be adequate for this purpose.

## Results and Discussion

Before presenting our results, we shall briefly review the molecular orbital (MO) analysis of simple biradicals such as 1.<sup>18</sup> Such structures are homosymmetric biradicals, in that the two p orbitals which contain the odd electrons are interconvertible by a symmetry operation of the molecule. Through-space overlap of these orbitals leads to two formally nonbonding MO's (NBMO): one symmetric with respect to a mirror plane and slightly bonding (S), the other antisymmetric and slightly antibonding (A). Energetically, S lies below A.

As first noted by Hoffmann,<sup>21</sup> the intervening methylene group (C2) in 1 provides a pair of orbitals — one bonding ( $\pi_{CH_2}$ ), one anti-bonding ( $\pi^*_{CH_2}$ ) — which can interact with the biradical orbitals. The A molecular orbital is prevented by symmetry from mixing with either of these orbitals, but the S molecular orbital can

mix with both. Interactions with the  $\pi_{\text{CH}_2}$  orbital increase the energy of the biradical S orbital, while interactions with the  $\pi^*_{\text{CH}_2}$  orbital decrease the energy. Generally, the former effect dominates, either because of a smaller energy gap between the orbitals or because of better overlap.<sup>22</sup> Since through-space effects place the S MO below the A MO, through-bond interactions can substantially diminish the S-A energy gap. However, if the through-bond interactions are much greater than the through-space effect, the magnitude of the S-A gap can actually increase, albeit with A below S.

The two MO's described above can be used to construct wavefunctions for the triplet and singlet states. In the high-spin species, the two electrons must occupy different orbitals, resulting in a simple, single-determinant wavefunction (1). Only for such a wavefunction does the term "orbital energy" have its usual meaning, and subsequent discussions of S-A energy gaps will always refer to triplet wavefunctions. For the singlet state three configurations are possible:  $\phi_S \phi_S$ ,  $\phi_S \phi_A$ , and  $\phi_A \phi_A$ . One of these ( $\phi_S \phi_A$ ) is forbidden by symmetry from mixing with the other two, and the lowest singlet is best described by the two-configuration MCSCF wavefunction (2).<sup>18</sup> The orbitals for this state must be optimized separately. Thus, in Eq. 2,  $\phi_S$  and  $\phi_A$  are the "natural orbitals" and their form very closely parallels that of the triplet MO's. The weighting of the configurations in this CI wavefunction is determined, for the most part, by the orbital energies. The configuration involving double occupation of the lower-energy orbital will generally have the larger CI coefficient, and the two configurations will have equal coefficients if the orbitals are degenerate.

$$^3\psi_{\text{RHF}} = (2)^{-1/2} (\phi_S \phi_A - \phi_A \phi_S) (\alpha\alpha) \quad (1)$$

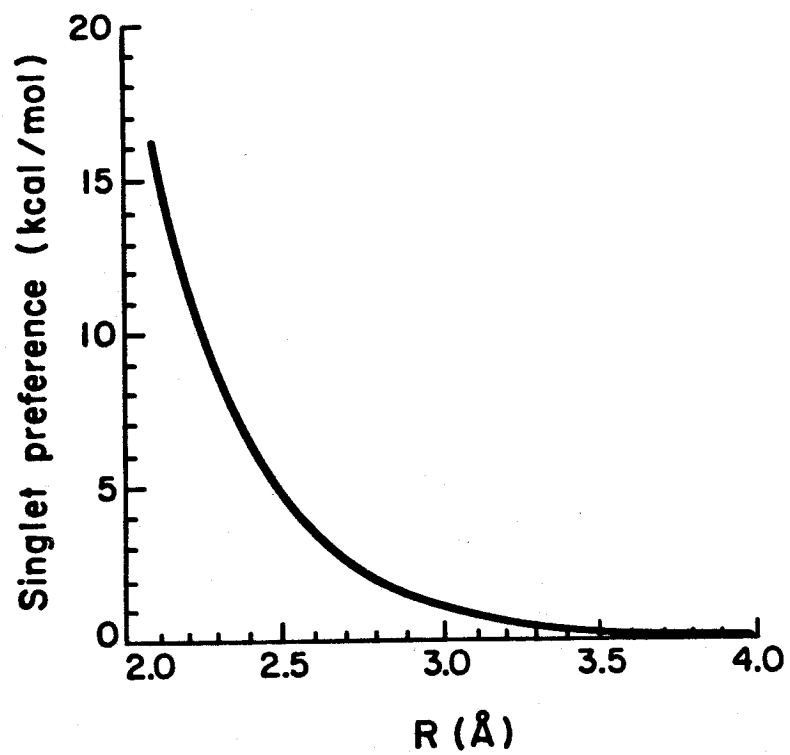
$$^1\psi_{\text{MCSCF}} = (C_1^2 + C_2^2)^{-1/2} (C_1 \phi_S \phi_S - C_2 \phi_A \phi_A) (\alpha\beta - \beta\alpha) \quad (2)$$

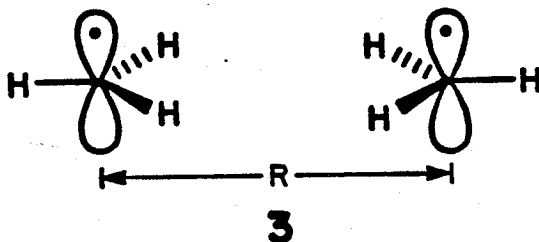
$$C_1, C_2 > 0$$

The value of the singlet-triplet gap ( $\Delta E_{\text{S-T}}$ ) depends upon two factors: (1) the energy difference between the S and A orbitals, with a large gap favoring the singlet; and (2) the exchange repulsion energy, which favors the triplet. The orbital energy gap will be large whenever either the through-space or the through-bond interaction dominates the other. In such cases a singlet ground state is expected. However, when the two effects are of comparable magnitude, a small S-A gap results. In this case it is difficult to predict the ground state multiplicity, but a triplet ground state is at least feasible.<sup>18</sup>

**Through-space Interactions.** We have modeled the through-space interactions<sup>21</sup> in localized biradicals such as **1** by considering two adjacent methyl radicals interacting in a  $\pi$  fashion (3,  $D_{2h}$  symmetry).<sup>23</sup> The results are shown in Fig. 1. At all separations,  $R$ , the radical pairs assume a singlet ground state. Evidently, the S-A gap dominates over the exchange repulsions even when  $R$  is large — just as in the case of  $\text{H}_2$ . What could be considered surprising about Figure 1 is the magnitude of the singlet preference. At a distance of 2.37 Å, corresponding to the separation in **1**,<sup>8</sup> singlet coupling is favored by a full 7.2 kcal/mole.

Figure 1. Singlet-triplet energy gap as a function of internuclear separation,  $R$ , for two weakly interacting methyl radicals (3).





A useful, alternative analysis of such interactions is provided by GVB theory, in which the radical electrons are confined to different orbitals which are optimized self-consistently.<sup>14</sup> The resulting GVB orbitals tend to localize on separate centers so that electron repulsions can be minimized. At the same time, these "left" and "right" orbitals ( $\phi_L$  and  $\phi_R$ ) also build in some density at the opposite centers. In this way, each one can reduce its kinetic energy without significantly affecting nuclear-electron attractions. A typical GVB pair is shown in Fig. 2.

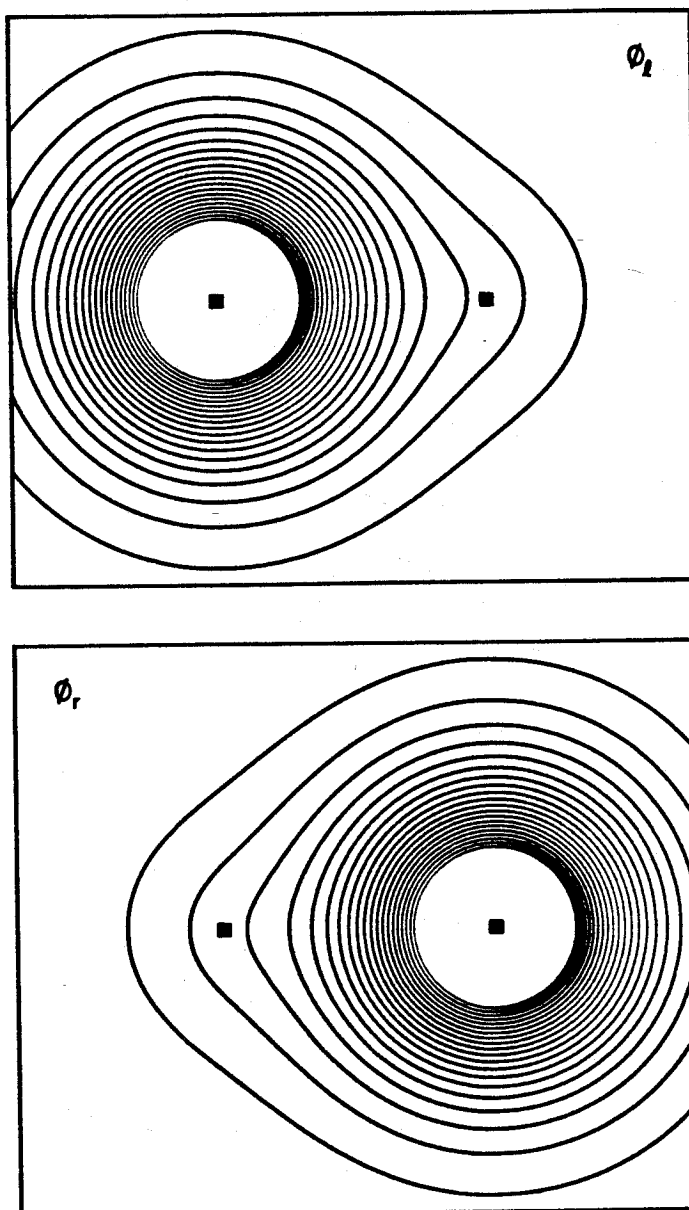
Singlet and triplet pairing of the GVB orbitals leads to wavefunctions (3) and (4), respectively. It can easily be shown that the singlet GVB wavefunction is equivalent to the MCSCF wavefunction (2), where the GVB orbitals are related to the natural orbitals by Eq. 5. The GVB pair overlap ( $S_{LR}$ ) is given by Eq. 6. The GVB orbitals are separately optimized for the triplet, and  ${}^3\psi_{\text{GVB}}$  and  ${}^3\psi_{\text{RHF}}$  can also be related by Eq. 5, with both  $C_1$  and  $C_2$  (which no longer represent CI coefficients) equal to 0.5. Notice that in this case, the overlap between the orbitals ( $S_{LR}$ ) is zero (Eq. 6).

$${}^1\psi_{\text{GVB}} = (2+2S_{LR}^2)^{-1/2} (\phi_L\phi_R + \phi_R\phi_L)(\alpha\beta - \beta\alpha) \quad (3)$$

$${}^3\psi_{\text{GVB}} = (2-2S_{LR}^2)^{-1/2} (\phi_L\phi_R - \phi_R\phi_L)(\alpha\alpha) \quad (4)$$

Figure 2. GVB Orbitals for two methyl radicals (3) at a distance of 2.37 Å. Contours indicate amplitudes of the orbitals 0.89 Å above the atomic plane. The increment between contours is 0.005 au. Amplitudes above 0.1 au have been omitted.

TWO METHYL RADICALS // R = 2.37  
GVB PAIR // OVERLAP = 2.0626D-01



$$\phi_l = (C_1^{1/2} \phi_S + C_2^{1/2} \phi_A) / (C_1 + C_2)^{1/2} \quad (5)$$

$$\phi_r = (C_1^{1/2} \phi_S - C_2^{1/2} \phi_A) / (C_1 + C_2)^{1/2}$$

$$S_{lr} = \frac{C_1 - C_2}{C_1 + C_2} \quad (6)$$

$$\Delta E_{S-T} = E_{GVB}^1 - E_{GVB}^3 =$$

$$\frac{4S_{lr} h_{lr} - 2S_{lr}^2 h_{ll} - 2S_{lr}^2 h_{rr} - 2S_{lr}^2 J_{lr} + 2K_{lr}}{1 - S_{lr}^4} \quad (7)$$

While Eq. 4 is the true high-spin GVB wavefunction, the triplet may be more conveniently approximated in the present systems by replacing the triplet-optimized  $\phi_l$  and  $\phi_r$  by the corresponding singlet GVB orbitals. This simplification allows each state to be described by a single configuration wavefunction involving the same set of orbitals, and this constitutes a major advantage of the GVB analysis of such wavefunctions. It also leads to a simple expression for  $\Delta E_{S-T}$  (Eq. 7),<sup>24</sup> where  $h$ ,  $J$ , and  $K$  are, respectively, the one-electron, Coulomb, and exchange integrals over the GVB orbitals. The first four terms in the numerator of Eq. 7 all depend explicitly on  $S_{lr}$ . Taken together, these terms are negative, so that increasing the overlap of the GVB pair favors the singlet. The fifth term,  $2K_{lr}$ , is always positive and thus favors the triplet. This result is in agreement with one's usual chemical intuition: a large overlap between the "left" and "right" orbitals indicates a bonding interaction and a strong preference for singlet spin multiplicity.

For the interaction in 3, the GVB orbital overlap is quite large

at short distances and a singlet ground state results. Increasing  $R$  decreases both  $S\rho_r$  and  $K\rho_r$ . Apparently,  $S\rho_r$  predominates at long distances just as it does at short distances, and the radical pair always remains a singlet. Thus, the MO and GVB analyses of through-space effects are quite similar.

**Through-bond Interactions in (0,0)-Trimethylene (4).** In order to model the interplay between through-space and through-bond effects, we have studied (0,0)-trimethylene (4) as a function of the C-C-C valence angle  $\theta$ . This species has been extensively studied theoretically,<sup>21,25</sup> although the singlet-triplet energy gap ( $\Delta E_{S-T}$ ) has not been a major emphasis of these investigations. As will be shown below 4 serves as an excellent model for 1.

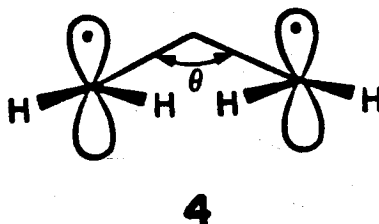


Figure 3 demonstrates that  $\Delta E_{S-T}$  in 4 is strongly dependent on  $\theta$ . The singlet is preferred at very large and very small values of  $\theta$ , while intermediate values lead to a triplet ground state.

Table I lists S-A orbital energy gaps for 3 and 4 as a function of  $R$ . The difference between these values is a reasonable estimate of the effect of through-bond coupling on the S-A gap. Clearly the dominant factor responsible for the variation in the S-A gap in 4 is the through-space overlap. To a first approximation, the through-bond effect is constant at 0.06 hartree, and the S-A gap in 4 can be

Figure 3. Singlet-triplet energy gap as a function of central angle,  $\theta$ , in (0,0)-trimethylene (4). Positive values indicate a singlet ground state.

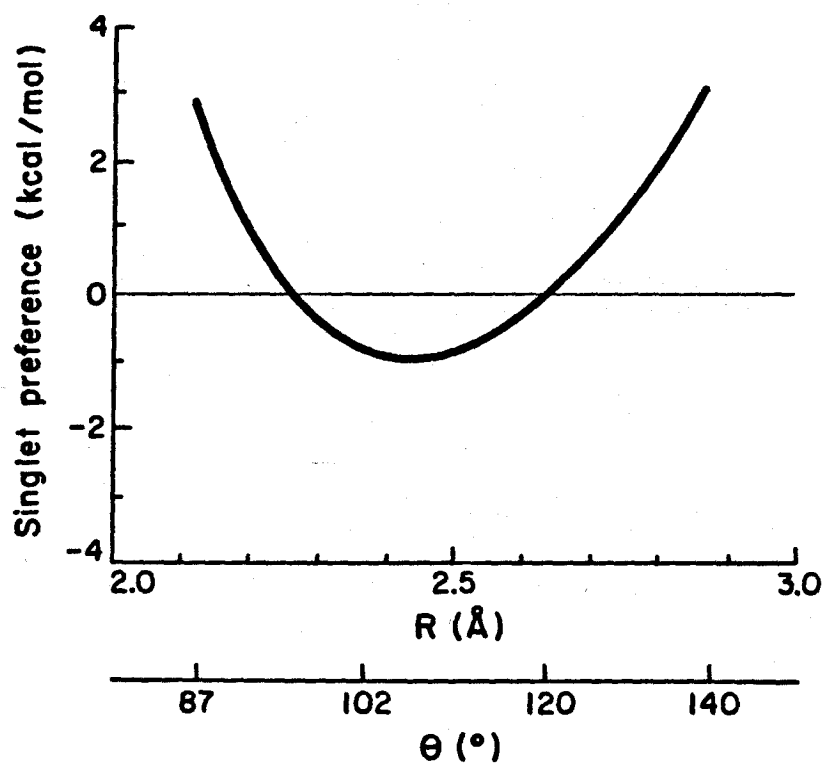


Table I. S-A Gaps and GVB Overlaps for 3 and 4

R(Å)	$\theta(^{\circ})^a$	S-A Gap (hartree)			$S/r$		
		3 <sup>b</sup>	4 <sup>b</sup>	Difference <sup>c</sup>	3	4	Difference <sup>c</sup>
2.12	87	0.085	0.031	0.054	0.299	0.160	0.139
2.25	95	0.069	0.011	0.058	0.240	0.086	0.154
2.37	102	0.057	-0.003	0.060	0.206	0.032	0.174
2.50	110	0.047	-0.016	0.063	0.164	-0.019	0.183
2.64	120	0.037	-0.030	0.067	0.132	-0.068	0.200
2.87	140	0.025	-0.051	0.076	0.092	-0.141	0.233

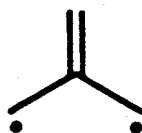
<sup>a</sup>Value of  $\theta$  in 4 which leads to the value of R shown. <sup>b</sup>A positive value indicates S below A. <sup>c</sup>Value for 3 minus the value for 4.

obtained by simply destabilizing the S orbital in 3 by this amount. Closer inspection reveals that the through-bond effect actually increases monotonically with increasing  $\theta$ . This is most likely a consequence of the fact that the coupling orbital at C2 is distorted toward the hydrogens, and thus overlap with the radical orbitals is greater at larger values of  $\theta$ .

The region in which 4 has a triplet ground state corresponds to the region of a small S-A gap. However, just a small S-A gap is not enough to produce a triplet ground state (Figure 1). Clearly, exchange repulsions must be substantial in such structures. This conclusion can be rationalized by extending Borden and Davidson's elegant treatment of singlet-triplet energy gaps in highly delocalized biradicals containing degenerate NBMO's.<sup>26</sup> For the through-space interaction in localized biradicals one can take appropriate linear combinations of the S and A orbitals and convert the NBMO's into two isolated p-orbitals. Thus, exchange repulsions in the singlet are small, and a singlet ground state is feasible. However, when the NBMO's of 4 are similarly treated, the through-bond coupling unit must always be present in each linear combination. As a result, exchange repulsions remain substantial in the singlet. In the structures studied by Borden and Davidson, such an effect necessarily induces a triplet ground state.<sup>26</sup> In 4, however, the NBMO's are not forced to be degenerate. Only when the through-bond and through-space effects nearly balance one another and the NBMO's are nearly degenerate does a triplet ground state result.

It seems likely that the more effective the through-bond coupling unit, the greater the exchange repulsions between NBMO's and the

greater the potential for a triplet ground state. In this light  $D_{3h}$  trimethylenemethane (5) can be viewed as a (0,0)-trimethylene with an especially effective through-bond coupling unit. Since the NBMO's of 5 are degenerate and "through-bond interactions" are quite large, a substantial energetic preference for the triplet ground state results.<sup>26,27</sup>

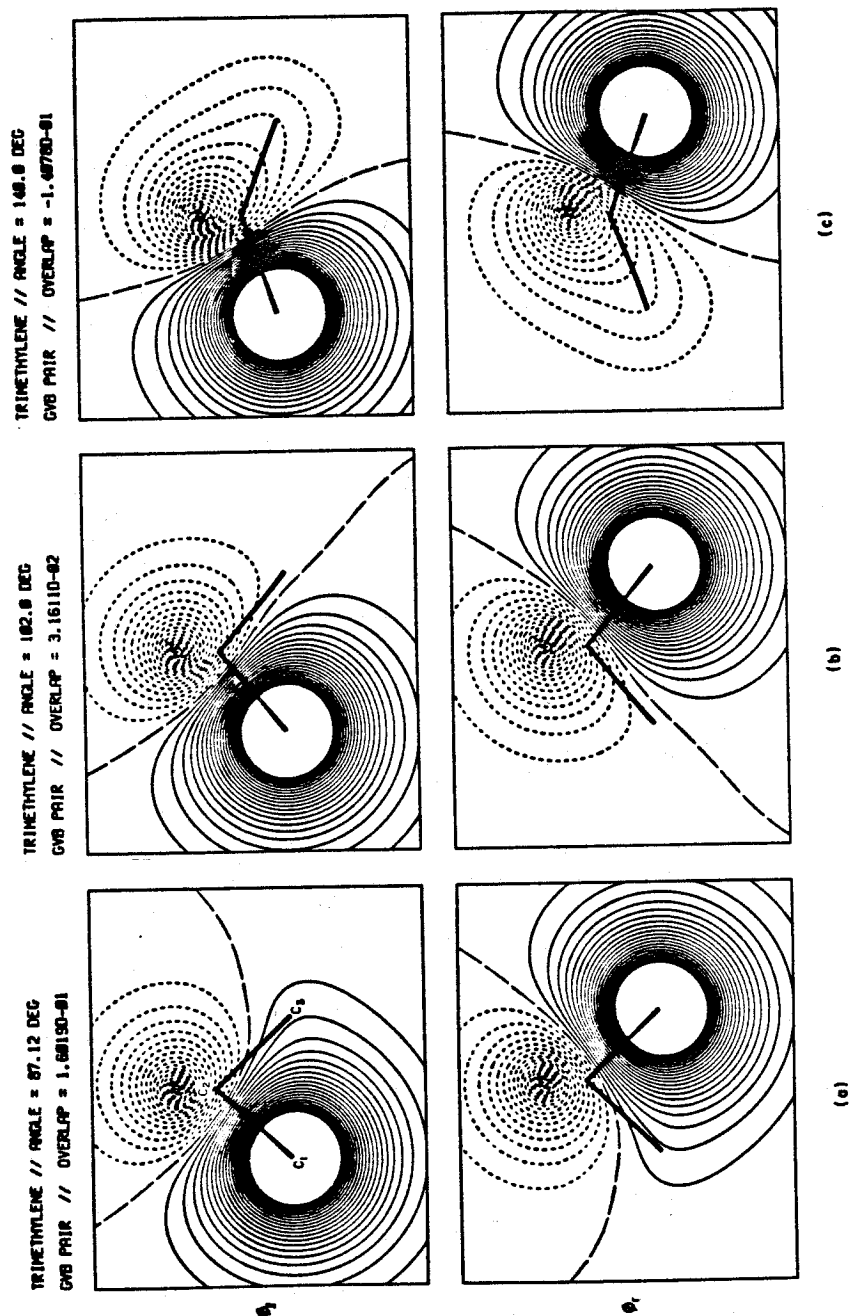


5

In GVB terms, when a through-bond coupling unit is introduced into a system, both  $\phi_l$  and  $\phi_r$  must become orthogonal to it.<sup>14</sup> As first pointed out by Goddard,<sup>14</sup> this is accomplished by incorporating the coupling unit out of phase, thus introducing a nodal surface into the GVB orbitals (Fig. 4). The sign at the "far" center in each orbital is then determined by a competition between through-space interactions, which favor having the two ends in phase, and the need to minimize one-electron energies. The latter effect favors having the "far" lobe in each orbital in phase with the through-bond coupling unit (i.e., out of phase with the main lobe).

When  $\theta$  is small, through-space overlap in 4 is large and the first effect dominates (Fig. 4a). However, when  $\theta$  is large, the second effect is more important, and the radical centers are out of phase in each GVB orbital (Fig. 4c). Thus, the position of the nodal surface changes in response to the variation in  $\theta$ . At intermediate

Figure 4. GVB Orbitals for three geometries of (0,0)-trimethylene (4), plotted as in Figure 2. Long dashes indicate nodes, while solid lines and short dashes indicate positive and negative amplitudes, respectively.



values, the node passes almost directly through the "far" center (Fig. 4b).

The way in which the GVB orbitals change with geometry has important implications on the extent to which they overlap with each other (Table I). If, by convention, the orbitals at C1 in  $\phi_l$  (C1(l)) and C3 in  $\phi_r$  (C3(r)) are assigned to be in phase (Fig. 4), the contribution to the overlap of the GVB pair ( $S_{lr}$ ) from the region of the through-bond coupling unit must be positive. The more important overlap, however, occurs where the AO coefficients are largest, and this is at the radical centers.<sup>28</sup> For small  $\theta$ , C1(l) and C3(l) are in phase, and thus C1(l) and C1(r) must also be in phase. Therefore, the GVB pair overlap at the radical centers reinforces the positive overlap at the through-bond coupling unit. As the central angle is opened (Fig. 4b), C1(l) and C3(l) become out of phase with respect to one another, and thus so do C1(l) and C1(r). The GVB pair overlap at the radical centers becomes negative, and this counterbalances the positive overlap at the through-bond coupling unit. The overall magnitude of  $S_{lr}$  is thus diminished and eventually  $S_{lr}$  goes to zero. Upon further expansion of  $\theta$ , the negative overlap at the radical centers overwhelms the positive overlap at C2, leading to a large, negative  $S_{lr}$  (Fig. 4c). The sign of the overlap, of course, has no true physical meaning. Thus, one is left with the counter-intuitive result that increasing the distance between the radical centers can actually increase the GVB pair overlap.

The quantitative trend in  $S_{lr}$  with varying  $\theta$  is shown in Table I. At all values of  $\theta$ ,  $S_{lr}$  in 4 is much less than in 3, as a result of through-bond coupling. As in our earlier analysis of the S-A MO

energy gap, the difference in  $S\rho_r$  between 3 and 4 can be taken as a measure of the effectiveness of through-bond coupling. The data indicate that through-bond coupling is more effective at larger values of  $\theta$ , again suggesting an enhanced overlap with C2 at large values of  $\theta$ .

Given the above analysis, it is now possible to consider the state splitting in trimethylene. Whenever the GVB overlap is large (greater than approximately 0.1) the singlet state should be lower in energy. This is precisely the case for  $\theta = 87^\circ$  or  $140^\circ$  (Fig. 3). At intermediate angles,  $S\rho_r$  approaches, and ultimately reaches zero. However,  $K\rho_r$  does not go to zero like it did in the through-space model system (3). This is because, when  $S\rho_r$  is diminished by special nodal properties of the GVB orbitals (as it is with through-bond coupling), the  $1/r$  term in  $K\rho_r$  necessarily leads to a finite positive value for the integral.<sup>29</sup> A triplet ground state thus results.

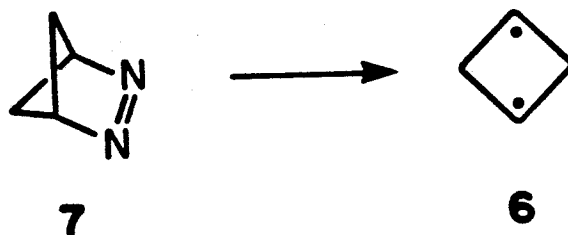
The similarity of the roles of  $S\rho_r$  in GVB theory and the S-A gap in MO theory is apparent. If either is diminished in absolute value by simply separating the radical centers, exchange repulsions are similarly diminished and a singlet ground state results. However, if special characteristics of the wavefunction cause  $S\rho_r$  or the S-A gap to fortuitously go to zero, the exchange repulsions can still be significant, and a triplet ground state may result. The reason for this parallel behavior is made clear with reference to Eq. 6.  $S\rho_r$  will be large whenever  $|C_1-C_2|$  is large, and, as discussed above,  $|C_1-C_2|$  will be large whenever the S-A gap is large. Note that just as Hund's rule for atoms predicts that whenever two electrons occupy two orthogonal orbitals on the same atomic center, the high spin state

is preferred, so the GVB analysis of molecules predicts that whenever the GVB pair orbitals occupy the same region of space and are orthogonal, or nearly so ( $S\rho_r \approx 0$ ), the high spin state is preferred.

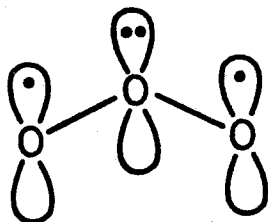
**Trimethylene Derivatives.** The discussion of 4 can easily be adapted to other 1,3-biradical systems. Several studies<sup>19,30</sup> have shown that ethano bridges are poor through-bond couplers. One would therefore expect that Closs' biradical (1), would resemble 4 with the appropriate value of  $\theta$  ( $102^\circ$ ).<sup>8</sup> Indeed, we find that the state splittings in 1 and 4 ( $\theta=102^\circ$ ) are 0.85 and 0.88 kcal/mol, at the current level of theory. Our original question concerning the reason for the triplet ground state in 1 is therefore answered.

In an attempt to observe the closely related structure 1,3-cyclobutadiyl (6), we have recently photolyzed azoalkane 7<sup>31</sup> at 8°K in a variety of matrices. However, we have been unable to observe any ESR signal corresponding to 6. Our calculations offer some insight into the reason for this failure. A reasonable geometry for 6<sup>32</sup> gives a 1...3 distance of 2.12 Å. From Figure 1, one can see that through-space effects at this distance lead to a singlet ground state, with the triplet a full 15.4 kcal/mol higher. Thus a fairly strong "π-bond" would exist in 6 if just through-space effects were operative. Through-bond coupling would be expected to oppose this "π-bond". Figure 3 shows that at the geometry corresponding to 6, (0,0)-trimethylene is also a singlet, but through-bond coupling has reduced the gap to 2.9 kcal/mol. Calculations on 6 itself reveal that the second methylene bridge further cancels the through-space effect, and the triplet becomes the ground state by 1.7 kcal/mol ( $S\rho_r=0.004$ ). Thus, our failure to observe 6 is not due to a singlet ground state,

but more likely reflects the triplet photochemistry of 7.<sup>33</sup> It would be interesting to devise alternative precursors to 6, and to design structures analogous to 6, but with very weak through-bond coupling units, to test for the existence of the '' $\pi$ -bond''.

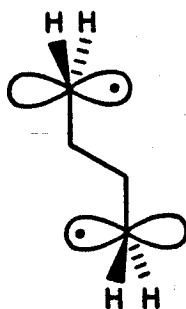


It is interesting in the present context to examine the inorganic biradical ozone (8), which is isoelectronic with 4. For a given separation, oxygen p-orbitals overlap less effectively than carbon orbitals, since they are more tightly held to the nucleus. Still, oxygen-centered radical pairs analogous to 3 exhibit singlet ground states.<sup>34</sup> Introduction of the central atom in 8 forces the two radical orbitals to become orthogonal to the central lone pair, which serves as a highly effective through-bond coupling unit.<sup>14</sup> The result, as in the case of 4, is a more negative value of  $S\rho_r$ . Since the system starts with only a very small overlap and the through-bond coupling is quite effective, the final absolute value of  $S\rho_r$  is large. Ozone thus has a strong preference for singlet spin multiplicity.<sup>14,35</sup>



8

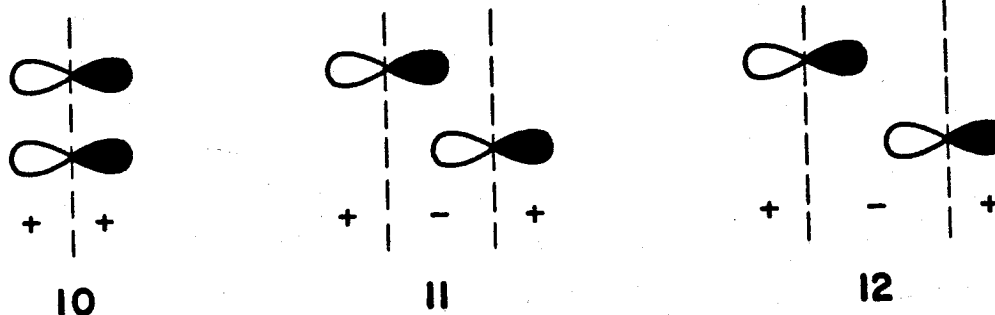
**Other Systems.** The approach described above for 1,3-biradicals can also be used to analyze other biradical systems. To illustrate this point, we shall consider the case of trans-(90,90)-tetramethylene (9).<sup>19,36</sup> It should be clear that similar reasoning can be applied to other systems.



9

Each GVB orbital arising from two methyl radicals interacting in the tetramethylene geometry<sup>19,36</sup> is essentially an atomic p-orbital localized at one of the radical centers.<sup>37</sup> The overlap of the two GVB orbitals is quite small ( $S_{\rho\rho}=0.003$ ). However, this result is due not only to the substantial distance between the centers, but also to the nodal properties of the orbitals. In fact, increasing the radical separation by moving one p-orbital along its axis yields an overlap

which is larger in magnitude. The reason for this apparent paradox can be seen in structures 10-12. In 10, two p-orbital are aligned in an appropriate arrangement for a  $\pi$  interaction. The nodes of the orbitals coincide, and the overlap is positive throughout all regions of space. As one of the p-orbitals is moved along its axis (11-12) a region of negative overlap is introduced between the two nodes. In 12, this negative overlap is greater than the positive overlap, indicating that the interaction is predominately  $\sigma$  in nature. Our calculations reveal that the through-space interactions in 9 correspond to structure 11, which is in the transition region between  $\sigma$  and  $\pi$  interactions. The very small through-space overlap thus results in part from a cancellation of overlaps. Since the nodal properties of the orbitals contribute significantly to their low overlap, one might expect that the exchange repulsions should predominate over  $S\rho_r$ , just as they did for the nearly orthogonal GVB orbitals of trimethylene with  $\theta=102^\circ$ . The radical pair would then exhibit a triplet ground state. Calculations reveal that this is, in fact, the case, but  $\Delta E_{S-T}$  is very small (0.07 kcal/mol), because the large separation of the radical centers forces  $K\rho_r$  to be small. Of course, this level of theory is not reliable for such small energy differences, but the results do illustrate an alternative mode by which triplet ground states can, in principle, be obtained.

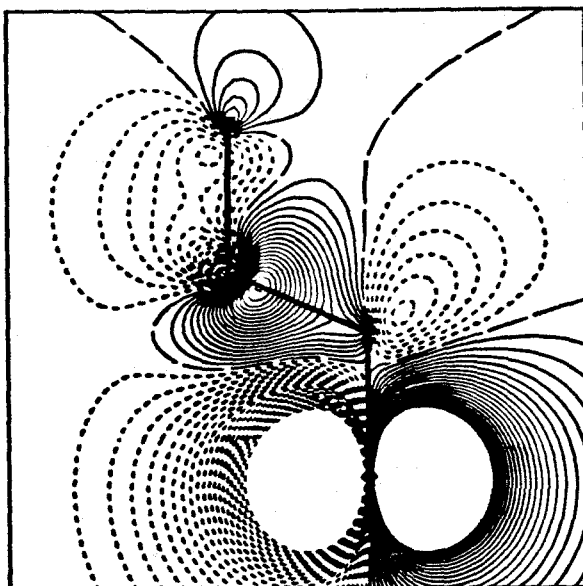
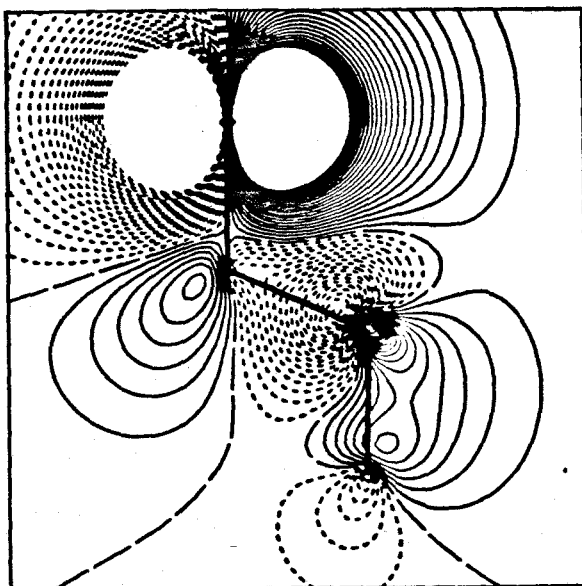


Introduction of the C2-C3 bond as a through-bond coupling unit in **9** once again causes each GVB orbital to incorporate that element in an antibonding way (Fig. 5). This induces a small contribution from the "far" centers, which are included in such a way as to minimize one-electron energies. Since there is no significant through-space overlap, the net result can only be an increase  $|S\rho_r|$ . It is worth noting that the sign of the overlap between the orbitals ( $S\rho_r$ ), as drawn in Figure 5, is positive, even though the overlap at the C2-C3 bond is negative. Evidently, the most important overlap occurs at the "ends" of the biradical, just as in the case of trimethylene (4). Because of the enhanced overlap from through-bond coupling in **9**, the system prefers the singlet state by 0.53 kcal/mol at the present level of theory. A recent study at the same level of theory but with an STO-3G basis set found that **9** has the largest singlet-triplet energy gap of any of the idealized forms of trans-tetramethylene.<sup>19</sup> The (0,90) form, in which the two p orbitals are orthogonal, has a very small preference for the triplet state, for reasons analogous to Hund's rule.<sup>19</sup> The (0,0) form, on the other hand, shows a very small preference for the singlet<sup>19</sup> because the ethano bridge is a very weak through-bond coupler.

Figure 5. GVB Orbitals for trans-(90,90)-tetramethylene (9).  
Contours are in the plane of the carbon atoms with plotting  
conventions as in Figures 2' and 4.

TETRAMETHYLENE

GVB PAIR // OVERLAP = 7.5891D-02



## Conclusion

It is now clear which factors are necessary for a simple biradical to have a triplet ground state. From Eq. 7, the most general requirement is that  $|S_{fr}|$  must be significantly smaller than  $K_{fr}$ . This can only be accomplished when  $S_{fr}$  is diminished by a cancellation of positive and negative regions of overlap,<sup>29</sup> rather than by a general reduction in overlap throughout all regions of space (as in 3 for long distances,  $R$ ). The cancellation may come about in a variety of ways. It may be forced by symmetry as in trans-(0,90)-tetramethylene. Alternatively, it may result from "accidental" nodal properties which have nothing to do with symmetry, as in the through-space interaction in 9. Finally, the cancellation may be caused by a precise balancing of through-bond and through-space interactions (1, 4, and 6).

Closs' biradical (1) falls into the third category and is thus a triplet due to a fortuitous balance of through-bond and through-space effects. The results of the present work would seem to significantly restrict the class of biradicals which will be observable under the conditions of the Closs experiment. Prime candidates still include 6 and related trimethylene derivatives.

In another connection, Doubleday has recently speculated that for localized (1,n) biradicals derived from Norrish Type I cleavage of cycloalkanones, the number of intervening  $\sigma$  bonds may influence  $\Delta E_{S-T}$ .<sup>12</sup> While we have not studied any structures which are directly relevant to Doubleday's work, our results do support the general notion since the effectiveness of through-bond coupling should depend

upon the number of intervening bonds. Note that for extended conformations of such structures, which would have very small through-space effects, through-bond interactions can only act to favor a singlet ground state.

**Acknowledgement.** We gratefully acknowledge the National Science Foundation (CHE-8024664) for support of this work. This work made use of the Dreyfus-NSF Theoretical Chemistry Computer, which was funded through grants from the Camille and Henry Dreyfus Foundation, the National Science Foundation (CHE-7820235) and the Sloan Fund of the California Institute of Technology. We especially thank Professor W.A. Goddard for helpful discussions and for access to the MQM library of programs. We are also indebted to John J. Low and Arthur F. Voter for their technical assistance. We also thank a referee for helpful comments.

## References and Notes

1. (a) Berson, J.A. In "'Rearrangements in Ground and Excited States, Vol. I'"; de Mayo, P., Ed.; Academic Press: New York, 1980; pp.311-390. (b) Gajewski, J.J. "'Hydrocarbon Thermal Isomerizations'"; Academic Press: New York, 1981. (c) Wagner, P.J. In "'Rearrangements in Ground and Excited States, Vol. III'"; de Mayo, P., Ed.; Academic Press, New York, 1980; pp. 381-444.
2. (a) Dowd, P. J. Am. Chem. Soc. **1966**, 88, 2587-2589. (b) Closs, G.L.; Kaplan, L.R., Bendall, V.I. Ibid. **1967**, 89, 3376-3377. (c) Arnold, D.R.; Evnin, A.B.; Kasai, P.H. Ibid. **1969**, 91, 784-785. (d) Berson, J.A.; Bushby, R.J.; McBride, J.M.; Tremelling, M. Ibid. **1971**, 93, 1544-1546. (e) Roth, W.R.; Erker, G. Angew. Chem. Int. Ed. Engl. **1973**, 12, 503-504. (f) Pagni, R.M.; Watson, C.R., Jr.; Boor, J.E.; Dodd, J.R. J. Am. Chem. Soc. **1974**, 96, 4064-4066.
3. Buchwalter, S.L.; Closs, G.L. J. Am. Chem. Soc. **1979**, 101, 4688-4694.
4. The term "'localized'" is used here in a classical sense, implying that the radical centers are not part of a conventional  $\pi$ -system. Of course, a major point of this work is that the radical centers do delocalize via the  $\text{CH}_2$  groups.
5. See Section III.
6. Closs, G.L., personal communication.
7. Of course, one must have a suitable photochemical precursor,

and it is quite possible that in some cases the photochemistry of the biradical precursor undermines the experiment (see below).

8. Conrad, M.P.; Pitzer, R.M.; Schaefer, H.F. III  
J. Am. Chem. Soc. **1979**, 101, 2245-2246.
9. Hund, F. Zs. Phys. **1925**, 33, 345-371. A new interpretation of Hund's Rule, in terms of anisotropic screening effects, has recently been offered: Shim, I.; Dahl, J.P. Theoret. Chim. Acta. **1978**, 48, 165-174.
10.  $S_0$  remains below  $T_1$  at all distances, even in much more sophisticated calculations: Kolos, W.; Wolniewicz, L.  
Chem. Phys. Lett. **1974**, 24, 457-460 and Alexander, M.H.; Salem, L. J. Chem. Phys. **1967**, 46, 430-439.
11. (a) Small, R.D., Jr.; Scaiano, J.C. Chem. Phys. Lett. **1977**, 50, 431-434. (b) Small, R.D., Jr.; Scaiano, J.C. J. Phys. Chem. **1977**, 81, 828-832. (c) Small, R.D., Jr.; Scaiano, J.C. Ibid. **1977**, 81, 2126-2131.
12. (a) Doubleday, C., Jr. Chem. Phys. Lett. **1979**, 64, 67-70.  
(b) Doubleday, C., Jr. Ibid. **1981**, 77, 131-134.  
(c) Doubleday, C., Jr. Ibid. **1981**, 79, 375-380.
13. Small singlet-triplet gaps generally lead to rapid intersystem crossing rates, due to favorable Franck-Condon factors.  
See, for example, Turro, N.J. "Modern Molecular Photochemistry"; Benjamin/Cummings: Menlo Park, California, 1978.
14. Goddard, W.A. III; Dunning, T.H., Jr.; Hunt, W.J.; Hay, P.J. Acct. Chem. Res. **1973**, 6, 368-376, and references cited therein.

15. Dunning, T.H., Jr. J. Chem. Phys. **1970**, 53, 2823-2833.
16. Huzinaga, S. J. Chem. Phys. **1965**, 42, 1293-1302.
17. All Hartree-Fock and two configuration SCF (i.e., GVB (1)) calculations were performed using the MQM: GVB2P5 program:  
Bair, R.A.; Goddard, W.A. III, unpublished work. Bair, R.A., Ph.D. Thesis, California Institute of Technology, 1982.  
Bobrowicz, F.W.; Goddard, W.A. III In ''Methods of Electronic Structure Theory''; Schaefer, H.F. III, Ed., Plenum Press: New York, 1977; pp. 79-127.
18. Salem, L.; Rowland, C. Angew. Chem., Int. Ed. Eng. **1972**, 11, 92-111.
19. Borden, W.T.; Davidson, E.R. J. Am. Chem. Soc. **1980**, 102, 5409-5410.
20. The CI calculation was carried out using the MQM: CI2P5 program:  
Bobrowicz, F.W.; Goodgame, M.M.; Bair, R.A.; Walch, S.P.; Goddard, W.A. III, unpublished work. Bobrowicz, F.W., Ph.D. Thesis, California Institute of Technology, 1974.
21. (a) Hoffmann, R. Acct. Chem. Res. **1971**, 4, 1-9.  
(b) Hoffmann, R. J. Am. Chem. Soc. **1968**, 90, 1475-1485.
22. Overlap appears to be the factor most responsible for favoring interactions with the  $\pi_{CH_2}$  orbital: Brunck, T.K.; Weinhold, F. J. Am. Chem. Soc. **1976**, 98, 4392-4393.
23. The C-H bond lengths in the two methyl radicals were chosen to be 1.09 Å.
24. This is actually the value for the ''triplet excitation energy''. The true value of  $\Delta E_{S-T}$  is obtained when the orbitals for each state (including the core orbitals) are

optimized separately. In the present systems, however, equation 7 very closely approximates  $\Delta E_{S-T}$ .

25. (a) Hay, P.J.; Hunt, W.J.; Goddard, W.A., III  
J. Am. Chem. Soc. **1972**, 94, 638-640. (b) Horsley,  
 J.A.; Jean, Y.; Moser, C.; Salem, L.; Stevens,  
 R.M.; Wright, J.S. Ibid. **1972**, 94, 279-282.
26. Borden, W.T.; Davidson, E.R. J. Am. Chem. Soc. **1977**, 99,  
 4587-4594.
27. This result is borne out by experiment<sup>2a</sup> and quantitative  
 theoretical calculations: Yarkony, D.R.; Schaefer, H.F., III  
J. Am. Chem. Soc. **1974**, 96, 3754-3758 and Davis,  
 J.H.; Goddard, W.A., III Ibid. **1977**, 99, 4242-4247.
28. There is ample precedent for the end overlaps being most  
 important: Hay, P.J., Ph.D. Thesis, California Institute of  
 Technology, 1972; pp. 68-71.
29. As shown below, the exchange integral,  $K_{\rho r}$ , depends explicitly  
 on the overlap function (f), as opposed to the overlap  
integral,  $S_{\rho r}$ , which is the integral of f over all space.

$$\begin{aligned}
 K_{\rho r} &= \iint \phi_{\rho}(1)\phi_r(1) \cdot (1/r_{12}) \cdot \phi_{\rho}(2)\phi_r(2) d\tau_1 d\tau_2 \\
 &= \iint f(1) \cdot (1/r_{12}) \cdot f(2) d\tau_1 d\tau_2
 \end{aligned}$$

At intermediate geometries of (0,0)-trimethylene, even though  $S_{\rho r}$  approaches zero, f does not. The integrand of  $K_{\rho r}$  is positive whenever f(1) and f(2) have the same sign and negative when they are oppositely signed. Most importantly, the integrand is,

in general, positive when the  $1/r$  term is greatest - namely when the two electrons are in the same region of space. Because of this fact,  $K_{\rho r}$  will be positive even when  $S_{\rho r}$  is zero.

30. Dixon, D.A.; Dunning, T.H., Jr.; Eades, R.A.; Kleier, D.A. J. Am. Chem. Soc. **1981**, 103, 2878-2880.
31. Chang, M.H.; Dougherty, D.A. J. Org. Chem. **1981**, 46, 4092-4093.
32. The geometry of the carbon framework was assumed to be identical to that in 1,3-dimethylenecyclobutane: Hemmersbach, P.; Klessinger, M.; Bruckmann, P. J. Am. Chem. Soc. **1978**, 100, 6344-6347.
33. Chang, M.H.; Dougherty, D.A. J. Am. Chem. Soc. **1982**, 104, 2333-2334.
34. The oxygen-centered radicals chosen for study were hydroxyl radicals. The calculations were performed with a double-zeta basis set.<sup>15,16</sup>
35. Closing down the central angle in ozone should make the triplet lower in energy than the singlet. However, another higher-lying state becomes the ground state as this distortion is made: Hay, P.J.; Dunning, T.H., Jr.; Goddard, W.A., III J. Chem. Phys. **1975**, 62, 3912-3914.
36. Segal, G.A. J. Am. Chem. Soc. **1974**, 96, 7892-7898.
37. There is a small amount of residual through-bond coupling through the C-H bonds, but this effect is negligible.

### Section III

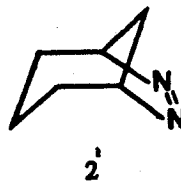
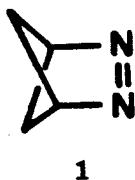
#### **Attempted Observation of the Cyclobutane- and Cyclohexane-1,3-Diyls**

### III. Attempted Observation of the Cyclobutane- and Cyclohexane-1,3-Diyls.

#### Introduction

The calculations in Section II show that at least part of the reason Closs' experiment<sup>1</sup> on the cyclopentane-diyl has not been extended to other localized biradical systems is that only a small fraction of these species exhibit the sensitive balancing of through-bond and through-space effects which is necessary to produce a triplet ground state. Nevertheless, one still might expect most simple 1,3-diyls to be observable by ESR. Unfortunately, the azo precursors to these biradicals have generally been synthetically inaccessible.

Over the last few years, this obstacle has been rapidly overcome. In 1980, Wilson<sup>2</sup> published a general synthesis for bicyclo[n.2.1] azo compounds with  $n \geq 2$ . More recently, Chang of this laboratory reported a method for making the remaining member of the series, with  $n=1$  (1).<sup>3</sup>



The present work was therefore undertaken to determine whether photolysis of any of these newly-available azo compounds might lead to ESR observation of the corresponding 1,3-diyls. The systems chosen for initial study were 1 and 2.

## Results and Discussion

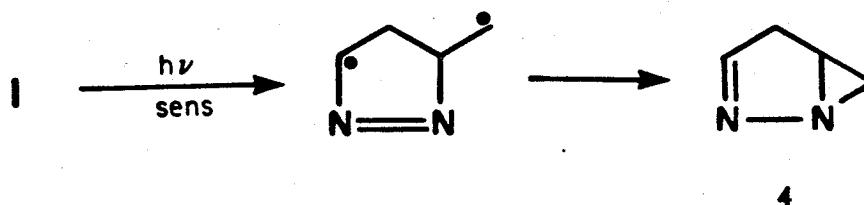
2,3-Diazabicyclo[2.1.1]hex-2-ene (1). When 1 is irradiated in a matrix at 8°K, a single, intense ESR peak is observed. It is believed that this signal arises from mono-radicals which are formed as azo-derived biradicals abstract hydrogen atoms from adjacent solvent molecules. Unfortunately, the broad nature of the hyperfine splittings precludes any more detailed analysis.



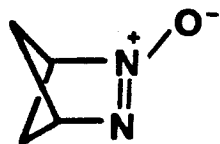
3

Of course, the absence of triplet resonances in the spectrum does not necessarily mean that 3 has a singlet ground state. More probably, it simply indicates that 1 is an unsuitable photochemical precursor for the triplet biradical. Chang<sup>3,4</sup> has shown that the triplet azo compound does not lose nitrogen, but undergoes  $\beta$ -cleavage to 4, instead (Scheme I). This rearrangement product, in fact, is the major product of photolysis at low temperature. The singlet azo compound, in contrast, does lose nitrogen. However, the resulting singlet biradical apparently closes before it has a chance to intersystem cross to the presumably lower-lying triplet.

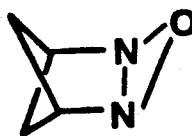
## Scheme I



**2,3-Diazabicyclo[2.1.1]hex-2-ene N-oxide (5).** In order to circumvent the unfortunate photochemistry of 1, an attempt was made to generate 3 through photolysis of the azoxy compound, 5. Previous studies by Michl<sup>5</sup> suggested that the major photoproduct of 5 would be the oxadiaziridine compound, 6. It was hoped, however, that a small amount of the compound would also lose N<sub>2</sub>O to give 3. Evidently this did not happen. A triplet signal could not be observed upon either direct or triplet-sensitized photolysis of 5. Moreover, analysis of the reaction mixtures provided no evidence of decomposition.



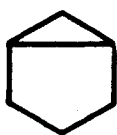
5



6

**2,3-Diazabicyclo[3.2.1]oct-2-ene (2).** Photolysis of 2 at 8°K in the ESR cavity failed to give either a triplet or a doublet signal. The azo compound did undergo decomposition, however. Analysis of the reaction mixtures revealed a total of three products: cyclohexane, cyclohexene, and a final one, which is believed to be bicyclohexane (7).<sup>6</sup>

The reason for the absence of any ESR signals is unclear, especially since the photochemistry of 2 has never been studied in detail. However, assuming the biradical 8 is formed, one might reasonably expect observation of this species to be complicated by its high degree of flexibility. Certain distortions of the biradical, for example, might facilitate closure to 7 by placing the radical orbitals in a conformation more conducive to intersystem crossing.<sup>7</sup> Furthermore, it is possible that the optimum biradical geometry might differ enough from the idealized (0,0)-trimethylene-like geometry to result in a singlet ground state for the system.



7



8

## Conclusion

It is now possible to appreciate how remarkable Closs' observation of the cyclopentane-diyl truly was. The calculations in Section II demonstrate that only a limited class of localized biradicals should exhibit a triplet ground state -- an important requirement for ESR observation of such species. The current work further shows that not all of even these few biradicals will be observable under the conditions of the Closs experiment. The precursor molecules must have the proper photochemistry (as **1** does not) and the biradicals may have to be somewhat rigid (as **8** apparently is not).

## Experimental

**2,3-Diazabicyclo[2.1.1]hex-2-ene (1) and 2,3-Diazabicyclo[2.1.1]hex-2-ene N-oxide (5).** These compounds were graciously provided by Moon Ho Chang of this laboratory.<sup>3</sup>

**2,3-Diazabicyclo[3.2.1]oct-2-ene (2).** This azo compound was synthesized by a modification of the literature procedures.<sup>2,8</sup> First, crude 5-hexenaltosylhydrazone was prepared in two steps from 5-hexen-1-ol (Pfaltz and Bauer), as described by Wilson.<sup>2</sup> The white solid was then dried for 12 hours under high vacuum before being used in the subsequent cyclization.

A 4.0 gm sample of crude tosylhydrazon<sup>1</sup>e was dissolved in 100 ml of dry CH<sub>2</sub>Cl<sub>2</sub>, and the solution cooled to 0°C under nitrogen. Upon

addition, by syringe, of 2.4 ml  $\text{BF}_3 \cdot \text{Et}_2\text{O}$  the mixture turned milky yellow in appearance. The solution was stirred for 4 hr. at  $0^\circ\text{C}$  and 48 hr. at room temperature, after which time the mixture was extracted (3x75 ml) with saturated sodium bicarbonate. The combined aqueous washings were extracted further with  $\text{CH}_2\text{Cl}_2$  (2x75 ml), and the combined organic extracts dried over  $\text{MgSO}_4$ . Removal of the solvent left a brownish-yellow paste which was purified by Kugelrohr distillation at  $90^\circ\text{C}$  and 0.01 torr. Separation of the azo compound from unreacted starting material was incomplete and accompanied by some decomposition, but yielded approximately 100 mg of 99.95% pure material.

**Preparation of ESR Samples.** Samples were prepared by dissolving the compound to be studied in enough purified solvent to make a 0.1 M solution. For the sensitization experiments, 0.25 mole/liter of either benzophenone or propiophenone was also added. The solutions were placed in 5 mm o.d. quartz ESR tubes (Wilmad) equipped with high vacuum stopcocks. The tubes were then degassed through three freeze-pump-thaw cycles and frozen in liquid nitrogen, before finally being inserted into the precooled ESR cavity.

**ESR Experiments.** A Varian E-9 spectrometer was outfitted with both an Air Products and Chemicals Helitran liquid helium transfer apparatus and an Oriel 200-W mercury-xenon lamp, which was focused into the microwave cavity. The output of the lamp, which was generally operated at 120-150W, was filtered through water, Pyrex, and, in the sensitization studies, a 365 nm cutoff filter.

The temperature at the sample was checked both periodically, with a calibrated thermocouple sealed in a sample tube, and continuously, with a less accurate thermocouple located 1 cm below the sample in the quartz Dewar. Heating above the minimum temperature (about 8°K) was achieved by adjusting either the helium flow rate or the Helitran automatic temperature controller.

**Analysis of Product Mixtures.** The product mixtures from 1 were analyzed, after warming, by gas chromatography on a column of 20''x1/8'' 10% UCW 982 on Chrom W, mesh size 80/100. Column temperature was maintained at 40°C and the gas flow kept at 128 cm<sup>3</sup>/min. The product mixtures from 2 were similarly analyzed on a column of 72''x1/8'' 5% OV-17 on Chrom P. Column temperature was kept at 50°C for 15 minutes and then increased to 110° at a rate of 20°/min. The gas flow was maintained at a constant 35 cm<sup>3</sup>/min.

## References and Notes

1. S.L. Buchwalter and G.L. Closs, J. Am. Chem. Soc., 101, 4688 (1979).
2. R.M. Wilson, J.W. Rekers, A.B. Packard, and R.C. Elder, J. Am. Chem. Soc., 102, 1633 (1980).
3. M.H. Chang and D.A. Dougherty, J. Org. Chem., 46, 4092 (1981).
4. M.H. Chang and D.A. Dougherty, J. Am. Chem. Soc., 104, 2333 (1982).
5. W.R. Dolbier, J., K. Matsui, H.J. Dewey, D.V. Horak, and J. Michl, J. Am. Chem. Soc., 101, 2136 (1979).
6. Detailed product studies were not performed, in part because the third product could not be easily separated from the cyclohexene. It was observed, however, that cyclohexene and the third product (presumably 7) were formed in nearly equal amounts. In addition, cyclohexane, only a minor product under conditions of direct photolysis, was the major product in the sensitization experiments.
7. For a review of orbital alignments which are favorable to intersystem crossing, see L. Salem and C. Rowland, Angew. Chem. Int. Ed., 11, 92 (1972).
8. A. Padwa and H. Ku, J. Org. Chem., 45, 3756 (1980).

#### Section IV

#### **ESR Studies of Spiropentane-based Rearrangements**

#### IV. ESR Studies of Spiropentane-based Rearrangements

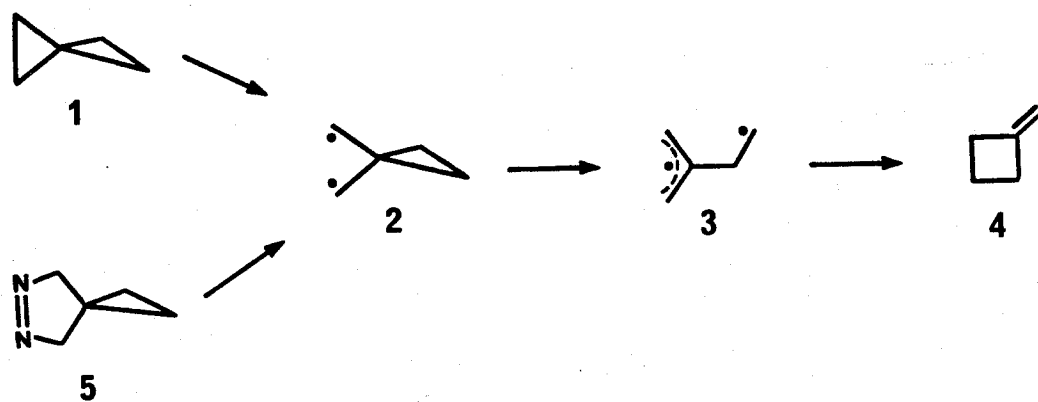
##### Introduction

One of the most intriguing possible fates of a localized biradical is its conversion to another biradical species — either localized or not. The most studied reaction of this type is probably the spiropentane rearrangement.<sup>1</sup> Thermolysis of spiropentane (1) leads to structural isomerization, as shown in Scheme I.<sup>2</sup> The first step in the reaction is known to be cleavage of a peripheral bond to form the cyclopropyldicarbonyl biradical, 2.<sup>3</sup> This process is presumably then followed by cleavage of a second bond to form the "allyl + p" biradical, 3,<sup>4</sup> which finally closes to methylenecyclobutane (4). The same pathway is apparently involved in the thermal decomposition of pyrazoline 5 (Scheme I).<sup>5</sup>

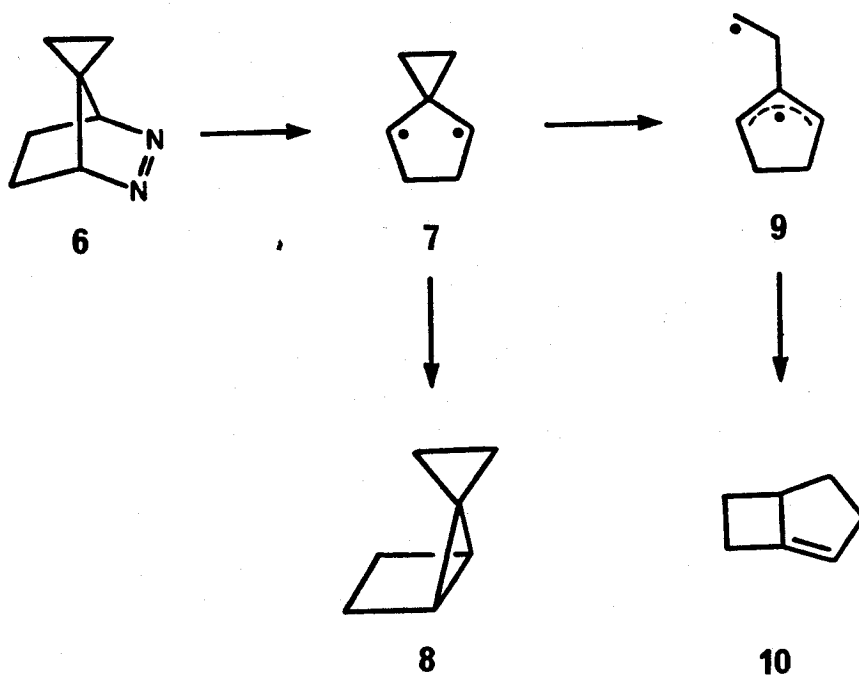
Modification of the spiropentane system by addition of an ethano bridge (6) leads to an almost identical sequence of events (Scheme II).<sup>6</sup> Both thermal and photochemical decompositions of 6 generate biradical 7, which can either close to 8 or rearrange, through biradical 9 to olefin 10. The ratio of the two products is highly dependent upon the spin state of the first-formed biradical, 7.<sup>7</sup> In the singlet manifold, closure to 8 is efficient, while in the triplet, closure is forbidden and rearrangement dominates.

Even though addition of a single ethano bridge only marginally alters the chemistry of the spiropentane system, McElwee-White of this laboratory has shown that addition of a second bridge dramatically changes the chemistry.<sup>8</sup> Thermolysis and direct photolysis of 11 both

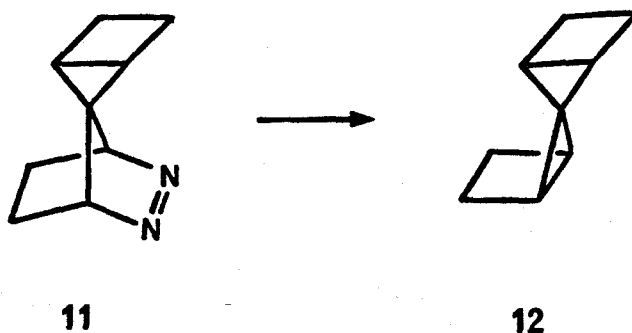
## Scheme I



## Scheme II

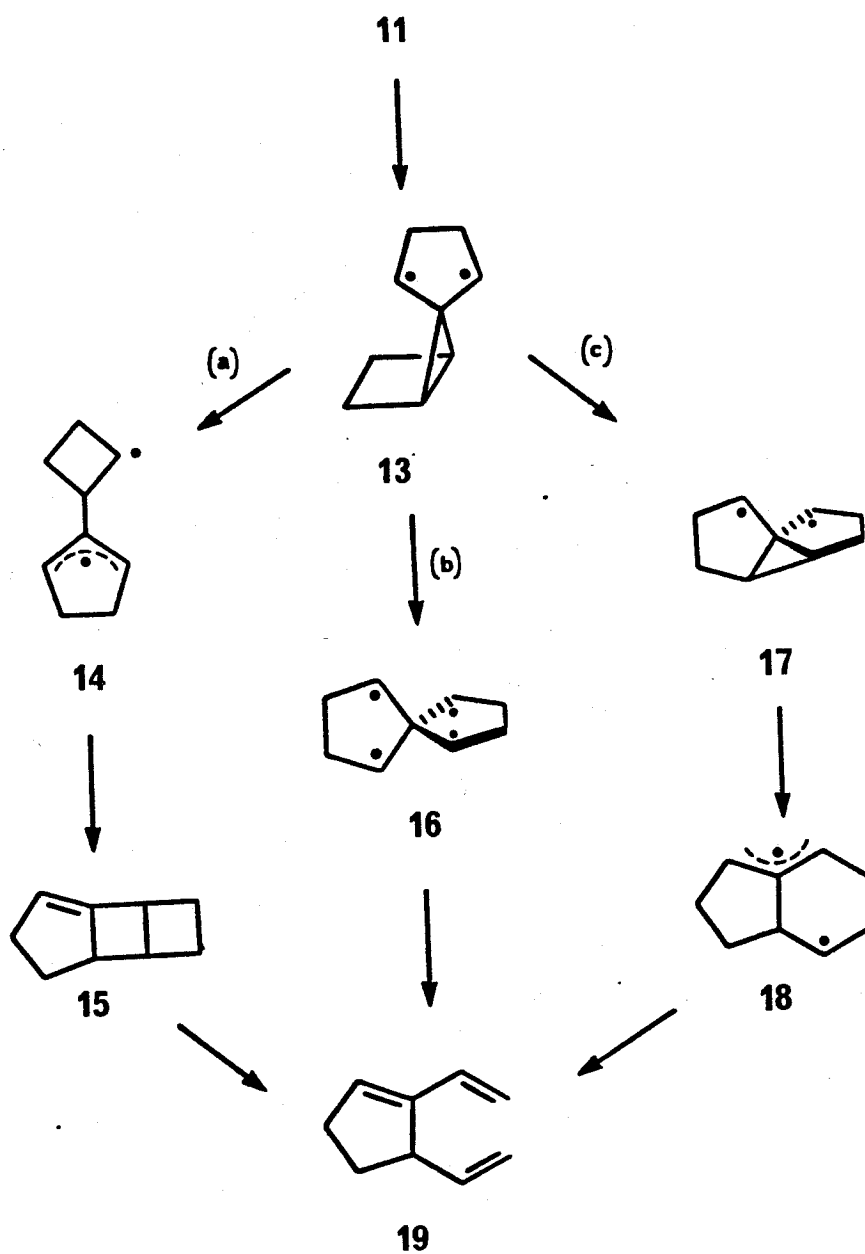


lead to the expected closure product 12. Triplet sensitized photolysis of the azo compound, however, yields divinylcyclopentene (19) as the major product. Deuterium labeling studies show that this product is formed by at least two, and perhaps as many as three parallel rearrangements of the first formed biradical, 13 (Scheme III). The conventional spiropentane rearrangement (path a) is known to be operative in this system, as is internal radical attack on the strained bicyclopentane bond (path c).<sup>9</sup> In addition, cleavage of the bicyclopentane bond to give the spiroconjugated tetraradical 16, may also take place.



Despite all the interest in these spiropentane-based rearrangements, remarkably little has been done to study the intermediate species directly. The present work was undertaken to see whether any of the triplet biradicals could be observed by ESR. Positive identification of any of these species would, by itself, be an important finding, and identification of more than one might permit a direct study of the interconversion between biradicals.

## Scheme III



## Results and Discussion

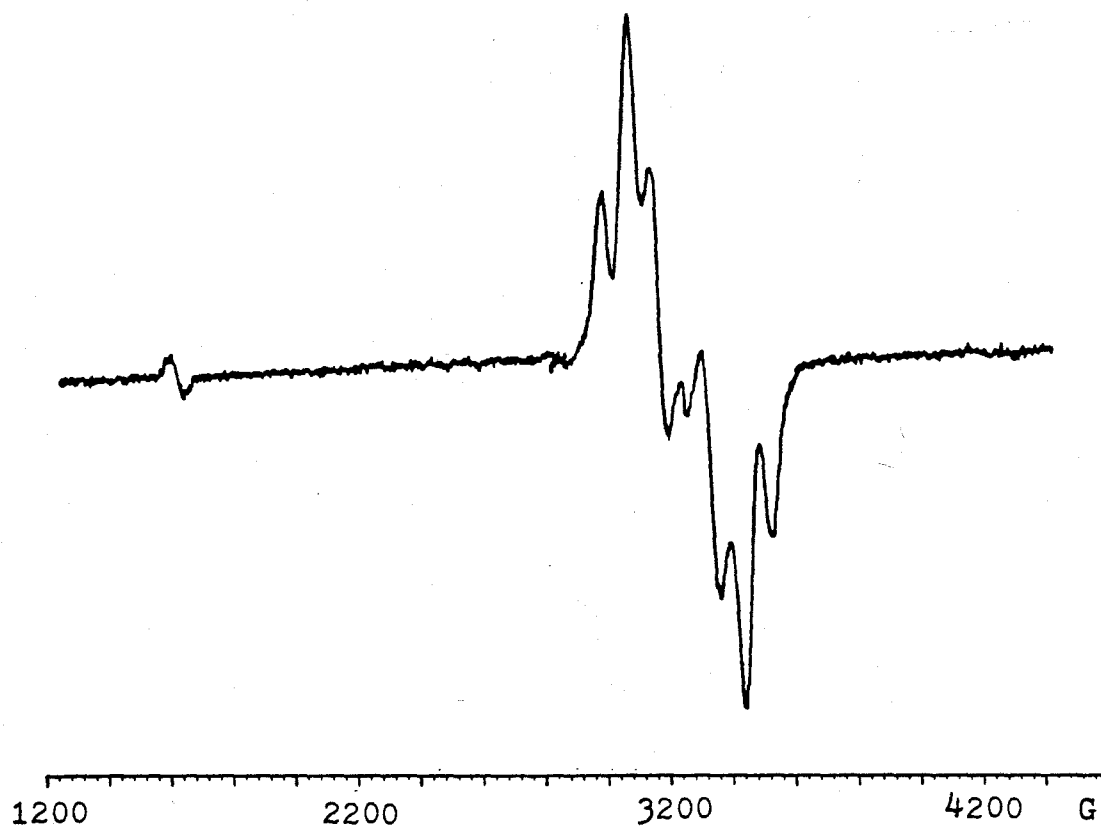
Irradiation of 11 in a glassy matrix of 2-methyl tetrahydrofuran<sup>10</sup> at 8°K leads to observation of the ESR spectrum shown in Figure 1. The general form of the signal — including the presence of a half-field,  $\Delta m_s = 2$  transition — suggests that it arises from a single triplet species.<sup>11</sup> The position of the  $\Delta m_s = 1$  transitions indicate zero-field splitting parameters of  $|D/hc| = 0.0255$  and  $|E/hc| = 0.003 \text{ cm}^{-1}$ . Almost identical values are found in the photolysis of 6.<sup>12</sup>

In order to identify the source of the two ESR signals, it is useful to compare the observed zero-field splitting parameters to those previously found in other organic biradicals. As shown in Table I, the observed D-values are much smaller than one would normally expect for a localized biradical such as 20. While this fact would seem to rule out the structurally related species, 7 and 13, as sources of the observed signals, it is possible that the cyclopropane ring in these compounds could allow the radical orbitals to delocalize enough to account for the lower values.

The extent to which this type of delocalization occurs has already been extensively studied by Roth.<sup>6</sup> He has shown that the bridge flip barrier in 21 is only 10 kcal/mole smaller than that in 22 — a difference which is easily explained in terms of the release of spiro strain in 21 which is not present in 22. For this reason it appears that there is no special electronic interaction between the cyclopropane ring and the radical orbitals. This conclusion is also supported by ab initio calculations of the zero-field splitting

Figure 1. ESR spectrum obtained upon irradiation of a 2-methyl tetrahydrofuran matrix containing 11 at 8°K.


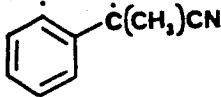
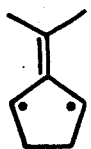
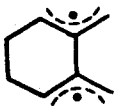
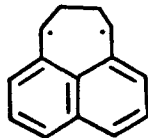

(a) Full Field spectrum



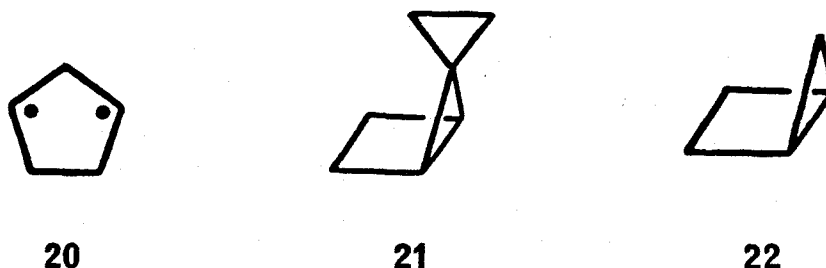
(b) Hyperfine structure on the  $\Delta m_s = 2$  peak



Table I. Zero-field splitting parameters for various biradicals<sup>16</sup>

Biradical	$ D/hc $ ( $\text{cm}^{-1}$ )	$ E/hc $ ( $\text{cm}^{-1}$ )
	0.024	0
	0.1069	0.0058
	0.027	0.0023
	0.0204	0.0016
	0.018	0.003
	0.084	0.0020

parameters. Even though introduction of the spiro-cyclopropane group does cause a noticeable reduction in the predicted D-value,<sup>13</sup> the effect is not large enough to account for the full experimental decline.



Another factor which militates against 7 and 13 as the currently observed triplet species is the persistence of the two ESR signals at high temperatures. The biradicals generated from both 6 and 11 are indefinitely stable at temperatures in excess of 85°K. In the first case, the biradical is even stable at 146°K.<sup>14</sup> Biradical 20, in contrast, has only a 15 minute half-life at 8°K.<sup>16</sup> Of course, it is possible that the cyclopropane moiety could perturb the system in such a way as to enhance the stability of the triplet state. For example, one would expect the tunneling reaction which accounts for most of the bicyclopentane (22) generated from 20 at low temperatures<sup>16</sup> to cease as the mass of the tunneling species is increased from 14 (for CH<sub>2</sub>) to 40 (for cyclopropane) or 66 (for "housane").<sup>16,17</sup> Still, this effect cannot explain the full stability of the unidentified triplets. The fact that decay is imperceptible at temperatures as high as 85°K or 146°K suggests that the E<sub>a</sub> for closure is at least 5 kcal/mole, and probably greater than 8 kcal/mol<sup>18</sup> — in either case significantly higher than 2.3 kcal/mole barrier reported for closure of 15.<sup>16</sup> It is

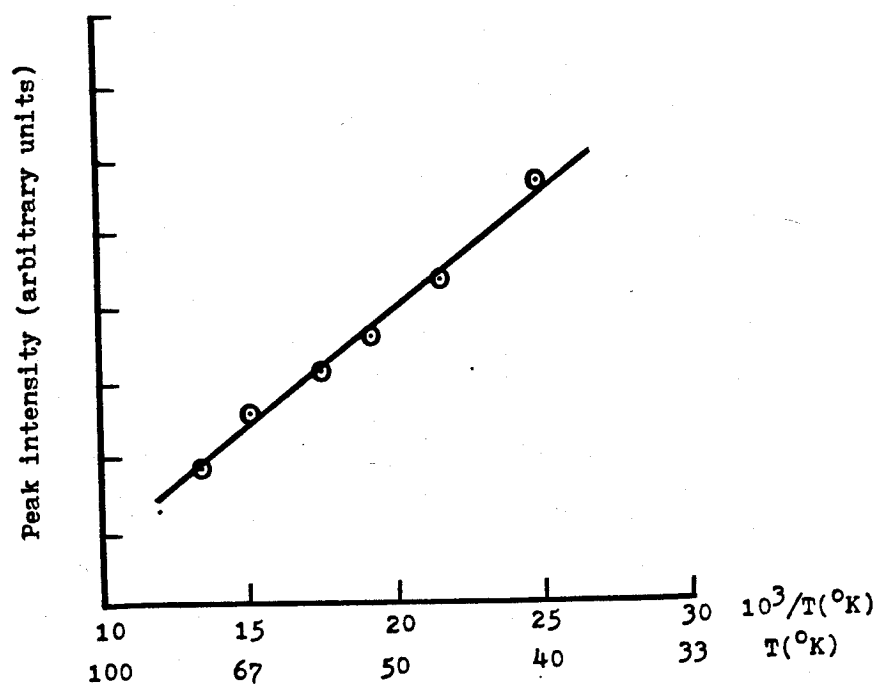
unclear exactly how the cyclopropane or ''housane'' group could cause such a dramatic increase.

While the first-formed biradicals, 7 and 13, appear to be unlikely sources of the ESR signals, the ''allyl+p'' biradicals that result from rearrangement of these species (9 and 14, respectively) seem to be much more viable candidates. Both of these species, for example, exhibit allylic resonance, which could account for the low observed D-values. This resonance (together with any interactions between the non-bonded allyl orbital and the non-conjugated p-orbital) might also help explain the persistence of the signals at high temperatures.

Other lines of reasoning, however, argue against these biradicals as the unidentified triplet species. For example, in order for the ESR signal to appear rapidly at 8°K, the C-C bond cleavage which takes 7 to 9 (or 13 to 14) would have to be unusually facile.<sup>19</sup> At the same time, the bond formation process that takes 9 to 10 (or 14 to 15) would have to be extremely slow, so that the signal could persist at high temperatures. This latter requirement seems particularly unattainable in the absence of any steric or orbital-alignment constraints to closure.

Even though the allyl+p biradical is the only triplet species to which 7 can rearrange, there are three alternatives in the case of biradical 13.<sup>8</sup> One is the spiroconjugated tetraradical 16. Unfortunately there are two lines of evidence which eliminate this species as a possible source of the ESR signal. First, a Curie plot of signal intensity versus inverse temperature<sup>11</sup> indicates that the observed biradical has a triplet ground state (Fig. 2). This result

Figure 2. Curie plot for the triplet species generated upon photolysis of 11. The corresponding plot for 6 has previously been reported.<sup>12</sup>



is in direct conflict with MC-SCF calculations which predict a singlet ground state for 16.<sup>20</sup> Second, the observed  $E/hc$  is not consistent with a species of  $D_{2d}$  symmetry.<sup>21</sup> Of course, the tetraradical might deviate from this symmetry to relieve the degeneracy of the non-bonding molecular orbitals. However calculations once again show that such a distortion is disfavored.<sup>20</sup>

Another possible rearrangement product from 13 is the localized biradical 17.<sup>8</sup> This species, however, is also an unlikely carrier of the triplet signal. Calculations of the zero-field splitting parameters using the point charge method<sup>22</sup> suggest that two p-orbitals in the appropriate geometry<sup>23</sup> should give a D-value which is much greater than the one observed (0.108 versus 0.0255  $\text{cm}^{-1}$ ).<sup>24</sup> Interactions with the cyclopropane ring might work to lessen this difference, but the geometry would seem to preclude any strong interactions.

The only remaining biradical which is known to play a role in the photochemistry and thermochemistry of 11 is another allyl+p biradical, 18.<sup>8</sup> As with the related species, 9 and 14, 18 would be expected to exhibit a low D-value and a high degree of thermodynamic stability. In addition 18 has a kinetically stabilizing factor: poor alignment between the radical orbitals and the C-C bond that must break as 18 is converted to 19. The chief problem with this species as the unidentified biradical is the lack of any corresponding intermediate from the other azo compound (6). It seems most reasonable that the two signals should arise from similar species.

The above discussion exhausts the list of biradicals which are currently believed to participate in the "'high'" temperature

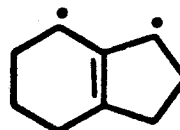
chemistry of 6 and 11. The low temperature chemistry of the compounds, however, may involve still other species. One particularly interesting set of possibilities consists of the trimethylenemethane (TMM) biradicals, 23, 24 and 25. These species correspond to the hydrogen shift products of 9, 14 and 18, respectively.<sup>25</sup> It is already known that TMM derivatives have zero-field splitting parameters almost identical to the ones currently observed (Table I). In addition, they have triplet ground states and are stable at elevated temperatures,<sup>26</sup> just like the unidentified biradical species. Of course, the TMM biradicals would be expected to lead to other products than 10 and 19.<sup>26</sup> However, the failure to observe new products at low temperatures does not rule out these species. The ESR technique is so sensitive that even a low level impurity could provide a strong signal.<sup>11</sup>



23



24



25

The extreme sensitivity of the method further raises the specter that untraceable azo impurities might be responsible for the ESR signals. Another conceivable danger is that the signals do not come from biradicals at all, but originate instead from triplet radical pairs that might be generated via biradical abstraction of solvent hydrogens. This seems highly unlikely, however. One would expect the wide distribution of matrix sites to prohibit the kind of extensive hyperfine structure observed on the  $\Delta m_s = 2$  peaks (Fig. 1b).

## Conclusions

The triplet species which are generated through the photolysis of 6 and 11 remain unidentified. Even though certain intermediates seem more likely candidates than others, none can be completely ruled out. Further experiments will undoubtedly have to be performed to resolve this issue.

## Experimental

7-(2,3-diazabicyclo[2.2.1]hept-2-ene)spirocyclopropane (6) and 7-(2,3-diazabicyclo[2.2.1]hept-2-ene)spiro-5'-bicyclo[2.1.0]pentane (11). The two azo compounds, synthesized as reported in the literature,<sup>6,8</sup> were graciously provided by Lisa McElwee-White of this laboratory.

**Preparation of ESR Samples.** Samples were prepared by dissolving the compound to be studied in enough purified solvent to make a 0.1 M solution. The solutions were placed in 5 mm o.d. quartz ESR tubes (Wilmad) equipped with high vacuum stopcocks. The tubes were then degassed through three freeze-pump-thaw cycles and frozen in liquid nitrogen, before finally being inserted into the precooled ESR cavity.

**ESR Experiments.** A Varian E-9 spectrometer was outfitted with both an Air Products and Chemicals Helitran liquid helium transfer apparatus and an Oriel 200-W mercury-xenon lamp, which was focused into the microwave cavity. The output of the lamp, which was generally operated at 120-150 W, was filtered through water and Pyrex.

Before each experiment, the temperature at the sample was checked with a calibrated thermocouple sealed in a sample tube. The temperature was then monitored throughout the experiment with a less accurate thermocouple fixed 1 cm below the sample in the quartz Dewar. Heating above the minimum temperature (about 8°K) was achieved by adjusting either the helium flow rate or the Helitran automatic temperature controller.

**Analysis of Product Mixtures.** The product mixtures were analyzed, after warming, by gas chromatography on a column of 20' x 1/8' 10% UCW 982 on Chrom W, mesh size 80/100. The gas flow rate was maintained at 50 cm<sup>3</sup>/min and the column temperature increased from 60°C to 200°C at 10°/min.

## References

1. For a recent review, see J.A. Berson, "Hypothetical Biradical Pathways in Thermal Unimolecular Rearrangements" in "Rearrangements in Ground and Excited States, Vol. I," P. de Mayo, ed. (New York: Academic Press, 1980).
2. M.C. Flowers and H.M. Frey, J. Chem. Soc. 5550 (1961);  
M.C. Flowers and A.R. Gibbons, J. Chem. Soc. B. 612 (1971).
3. J.J. Gajewski, J. Am. Chem. Soc., 92, 3688 (1970);  
J.J. Gajewski and L.T. Burka, ibid., 94, 8857 (1972).
4. The same "allyl+p" biradical has been invoked in the thermal interconversion of 4,4- and 2,2-dideuteriomethylene-cyclobutane: W. von E. Doering and J.C. Gilbert, Tet. Suppl., 7, 397 (1966).
5. K.K. Shen and R.G. Bergman, J. Am. Chem. Soc., 99, 655 (1977).
6. W.R. Roth and K. Enderer, Liebigs Ann. Chem., 733, 44 (1970).
7. "First formed" biradical is meant to imply the first formed hydrocarbon biradical. A diazenyl biradical may, of course, precede such a species.
8. L. McElwee-White and D.A. Dougherty, J. Am. Chem. Soc., in press.
9. Internal radical attack may actually be taking place in two different modes. Backside attack is known to occur, and frontside attack may also participate. In either case, the unlabeled compound gives the same biradical, 17.
10. Other matrices, such as perfluorobenzene and 2-methylpentane:

3-methylpentane 1:1, gave similar spectra, as did a polycrystalline powder of the azo compound. However, in these cases the signal was not as strong and was partially obscured by a large doublet peak.

11. J.E. Wertz and J.R. Bolton, Electron Spin Resonance: Elementary Theory and Practical Applications (New York: McGraw-Hill, 1972).
12. D.M. Lokensgard and J.A. Berson, unpublished results.
13. Calculations using the program described in Section V predict D-values of  $0.124 \text{ cm}^{-1}$  for 20 and  $0.101 \text{ cm}^{-1}$  for 13. The input singly-occupied molecular orbitals were obtained from Restricted Hartree-Fock (RHF) calculations on the two biradicals, performed with basis sets of double-zeta quality. The geometry of the five-membered ring in both systems was fixed as previously optimized by Schaefer: M.P. Conrad, R.M. Pitzer, and H.F. Schaefer III, J. Am. Chem. Soc., **101**, 2245 (1979). The geometry of the cyclopropane ring in 13 was optimized by MNDO. This optimization, as well as the RHF calculation on 13, was performed by Lisa McElwee-White:
14. Since glasses composed of 2-methyl tetrahydrofuran permit diffusion over 85°K, stability of the triplet species at higher temperatures had to be tested in another solvent — propylene glycol. Temperatures greater than 146°K were not used due to both the limitations of the Helitrans apparatus and the expected softening of the matrix at higher temperatures.<sup>15</sup> Compound 11 was never photolyzed in

propylene glycol, so its stability at high temperatures is still uncertain.

15. G. Fischer and E. Fischer, Molecular Photochemistry, 8, 279 (1977).
16. S.L. Buchwalter and G.L. Closs, J. Am. Chem. Soc., 101, 4688 (1979).
17. Closs has shown that merely increasing the mass of the tunneling species from 12 (for CH<sub>2</sub>) to 14 (CD<sub>2</sub>) substantially retards the tunneling reaction.
18. This estimate is based on a pre-exponential factor identical to that observed by Closs (i.e., 10<sup>8</sup> s<sup>-1</sup>).<sup>16</sup>
19. The Arrhenius parameters for a conventional cyclopropylcarbinyl to allylcarbinyl rearrangement are log A=12.48 and E<sub>a</sub>=5.94 kcal/mole: B. Maillard, D. Forrest, and K.U. Ingold, J. Am. Chem. Soc., 98, 7024 (1976).
20. L. McElwee-White, W.A. Goddard III, and D.A. Dougherty, manuscript in preparation.
21. E/hc is directly proportional to the energy difference between the 'x' and 'y' magnetic substates at zero field.<sup>11</sup> In systems with D<sub>2d</sub> symmetry, these two substates should be degenerate and E/hc should be zero.
22. For a general discussion of the method, see R. McWeeney, J. Chem. Phys. 34, 339 (1961), or A. Pullman and E. Kochanski, Int. J. Quant. Chem., 251 (1967). The program used in these studies was an adaptation of the one developed by D.A. Dougherty and J.A. Berson (unpublished work).
23. The two interacting orbitals were assumed to be unperturbed

from their position in the tetraradical. The geometry of the tetraradical was taken from reference 19. <sup>20</sup>

24. For comparison, the same type of calculation predicted a D-value for cyclopentane-diyl of  $0.138 \text{ cm}^{-1}$ , compared with an experimental value of  $0.084 \text{ cm}^{-1}$ .
25. It should be pointed out that 1,2-hydrogen shifts have never been proven to occur in radical species.
26. J.A. Berson, Acct. Chem. Res., 11, 446 (1978).

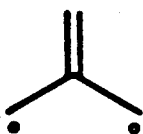
Section V

**Development of a Computer Program for  
Calculating Zero-field Splitting Parameters  
in Localized Biradicals**

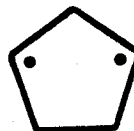
**V. Development of a Computer Program for  
Calculating Zero-field Splitting Parameters  
in Localized Biradicals.**

**Introduction**

The zero-field splitting parameters obtained from ESR spectra serve as a convenient means for recognizing particular triplet biradicals.<sup>1</sup> Indeed, the identification of new species is frequently facilitated by the comparison of experimental D- and E-values with the ones previously observed for other biradicals. Obviously, it would be quite useful if the same values could be calculated from first principles.



1

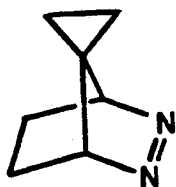


2

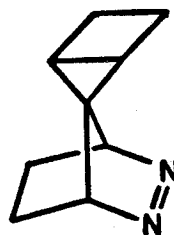
This problem has generated considerable theoretical interest over the past 20 years.<sup>2-7</sup> The parameters for delocalized biradicals such as trimethylenemethane (1) have been calculated several times with varying degrees of success.<sup>2-7</sup> Unfortunately, one of the major obstacles in these systems is the inability of a single-determinant wavefunction to adequately describe the distribution of electron spin.<sup>2,3</sup> Of course, the same problem would not be as pronounced in the case of a localized biradical.<sup>8</sup> However, calculations on a

triplet of this type have never been performed.<sup>9</sup> The reason for this "oversight" is not difficult to understand; the first localized biradical was not observed until 1975<sup>10</sup> and this species, cyclopentadiyl (2), remains the only one seen to date.<sup>11</sup>

The present work was therefore undertaken to develop a program for calculating the zero-field splitting parameters in localized biradicals. It was hoped that these efforts would complement the experimental work described in Sections III and IV. In practice, the program has proved quite useful in assessing the chances that various species might be responsible for the ESR signal that is obtained upon photolysis of 3 and 4.<sup>12</sup>



3



4

### Overview of Various Possible Approaches

The zero-field splitting parameters of a triplet species are related to the energies of the three magnetic sublevels at zero magnetic field. The non-degeneracy of these levels results from dipole-dipole coupling between the spins of the unpaired electrons. This interaction can be described in terms of a tensor,  $D$ , as shown in Eq. 1.

$$D = \frac{g^2 \beta^2}{2} \begin{bmatrix} \frac{x^2 - 3y^2}{r^5} & \frac{-3xy}{r^5} & \frac{-3xz}{r^5} \\ \frac{-3xy}{r^5} & \frac{x^2 - 3z^2}{r^5} & \frac{-3yz}{r^5} \\ \frac{-3xz}{r^5} & \frac{-3yz}{r^5} & \frac{x^2 - 3y^2}{r^5} \end{bmatrix} \quad (1)$$

The elements of  $D$  must be averaged over the electronic wavefunction,  $\Psi$ , which is simply an antisymmetrized linear combination of the two singly occupied molecular orbitals,  $\psi_a$  and  $\psi_b$  (Eq. 2). For this reason, the expectation value for each of the operators,  $\hat{O}$ , can be written as in Eq. 3.

$$\Psi = 2^{-1/2}(\psi_a\psi_b - \psi_b\psi_a) \quad (2)$$

$$\begin{aligned} \langle \Psi | \hat{O} | \Psi \rangle &= (1/2) \langle (\psi_a\psi_b - \psi_b\psi_a) | \hat{O} | (\psi_a\psi_b - \psi_b\psi_a) \rangle \\ &= \langle \psi_a\psi_b | \hat{O} | \psi_a\psi_b \rangle - \langle \psi_a\psi_b | \hat{O} | \psi_b\psi_a \rangle \end{aligned} \quad (3)$$

Once Eq. 3 is evaluated for each  $\hat{O}$ ,  $D$  may be diagonalized to give  $d_D$ . The diagonal elements of this matrix are the energies of the three magnetic sublevels. The one with the largest absolute value is typically multiplied by a factor of 1.5 to give the scalar zero-field splitting parameter,  $D$ . The difference between the other two elements, in contrast, is multiplied by 0.5 to give  $E$ .<sup>1</sup>

The problem of calculating  $D$  and  $E$  thus becomes one of evaluating the integrals in Eq. 3. This can be accomplished in a number of

different ways. First, the integrals may be solved for analytically. This approach has already been employed successfully in the study of delocalized  $\pi$ -systems.<sup>2-4</sup> Unfortunately, most of the formulas needed to compute the integrals in localized systems have not yet been derived.

An alternative method involves the simulation of basis atomic orbitals by a small number of point charges: one for each s-orbital and two for each p-orbital. This technique has proved quite reliable in delocalized systems,<sup>5-7</sup> but it, like the analytical approach, cannot be easily modified for localized biradicals. Calculations show that the D- and E-values predicted for species of this type are strongly dependent on the source of the triplet wavefunction (Table I)<sup>13</sup> — a complication which does not arise in delocalized systems.<sup>14</sup> In addition, the technique cannot properly handle contributions from more than a single orbital on each atomic center. This, of course, is a prerequisite for treating hybrid orbitals and orbitals which do not lie along a coordinate axis.

A final approach is to approximate the two electron distributions ( $\psi_a$  and  $\psi_b$ ) not by a few point charges, but by hundreds or thousands of them. The result is then essentially a numerical evaluation of the integrals. Once again, this method has only been used with delocalized systems in the past.<sup>3</sup>

### The Numerical Integration Method

Numerical computation of the integrals in Eq. 3 can be viewed as an approximate method in which the two orbitals,  $\psi_a$  and  $\psi_b$ , are

**Table I.** Zero-field splitting parameters calculated for 2  
using the point charge method.<sup>13</sup>

Source of Wavefunction	$ D/hc $	$ E/hc $
HMO	0.138 cm <sup>-1</sup>	0.008 cm <sup>-1</sup>
MNDO	0.056	0.012
RHF	0.067	0.016
UHF	0.070	0.011
[experimental values]	0.084	0.002

expanded in terms of box-like basis functions (Eq. 4). In this scheme, the coefficients of the basis functions correspond to the amplitudes of the orbitals in the appropriate boxes. When the orbital expansions are substituted into Eq. 3, the result is Eq. 5.<sup>15</sup>

$$\psi_a = \sum_i c_{ai} \phi_i \quad \psi_b = \sum_j c_{bj} \phi_j \quad (4)$$

$$\begin{aligned} \langle \Psi | \hat{O} | \Psi \rangle &= \left\langle \sum_i c_{ai} \phi_i \sum_j c_{bj} \phi_j \right| \hat{O} \left| \sum_k c_{ak} \phi_k \sum_l c_{bl} \phi_l \right\rangle \\ &= \left\langle \sum_i c_{ai} \phi_i \sum_j c_{bj} \phi_j \right| \hat{O} \left| \sum_k c_{bk} \phi_k \sum_l c_{al} \phi_l \right\rangle \quad (5) \end{aligned}$$

Since the box-like basis functions do not overlap at any point in space, only integrals with  $i=k$  and  $j=l$  need be considered. Thus Eq. 5 reduces to Eq. 6. For a given  $i, j$  pair of basis orbitals, the contribution to the total integral is given by Eq. 7. The term in brackets is a weighting coefficient which depends upon the amplitudes within the boxes, while the integral is a quantity which is determined by the distance between the boxes. Both expressions are easily evaluated, and the various  $\phi_{ij}$ 's need only be added together to arrive at the final integral in Eq. 3.

$$\begin{aligned} \langle \Psi | \hat{O} | \Psi \rangle &= \left\langle \sum_i c_{ai} \phi_i \sum_j c_{bj} \phi_j \right| \hat{O} \left| \sum_i c_{ai} \phi_i \sum_j c_{bj} \phi_j \right\rangle \\ &= \left\langle \sum_i c_{ai} \phi_i \sum_j c_{bj} \phi_j \right| \hat{O} \left| \sum_i c_{bi} \phi_i \sum_j c_{aj} \phi_j \right\rangle \quad (6) \end{aligned}$$

$$\begin{aligned}
\theta_{ij} &= (C_{ai}C_{bj})^2 \langle \theta_i \theta_j | \hat{O} | \theta_i \theta_j \rangle - (C_{ai}C_{bj}C_{bi}C_{aj}) \langle \theta_i \theta_j | \hat{O} | \theta_i \theta_j \rangle \\
&= [(C_{ai}C_{bj})^2 - (C_{ai}C_{bj}C_{bi}C_{aj})] \langle \theta_i \theta_j | \hat{O} | \theta_i \theta_j \rangle
\end{aligned} \tag{7}$$

### Programming Considerations

Each of the integrals in Eq. 3 is a sum over a six-dimensional space (three dimensions for each electron). Consequently, the total number of contributions ( $\theta_{ij}$ ) which must be added together is  $N^6$ , where  $N$  is the number of boxes in the space along one direction. Of course it is imperative that the number of operations which are actually executed this many times be kept to a minimum. Only in this way can a calculation be limited to a reasonable amount of time.

There are three basic tasks which must be performed in the evaluation of the  $\theta_{ij}$ 's: 1) computation of the amplitudes within the box-like basis orbitals; 2) evaluation of the weighting coefficients; and 3) calculation of the integrals between boxes. The first of these need only be executed two times within Cartesian space -- once for each orbital -- for a total of  $2N^3$  times. The second, however, must be carried out the full  $N^6$  times, since the weighting coefficients depend upon the coordinates of both electrons. Finally, the third operation, calculation of the integrals between boxes, has to be performed once for every unique vector linking two boxes. Several  $i, j$  pairs will obviously have the same vector joining them, and it can be shown that the total number of unique vectors is only  $(2N-1)^3$ .<sup>16</sup>

The figures above represent the number of times that each computation must be carried out in the most general case. In

molecules with symmetry, however, these values can be reduced substantially. For example, if the amplitudes, weighting coefficients, or basis set integrals are the same in different regions of space, only a fraction of these quantities need to be separately evaluated.<sup>17</sup> Moreover, certain of the D-tensor elements may be forced to zero, depending upon the type of symmetry present.<sup>18</sup> All of these factors can be useful in making the calculations of the integrals as efficient as possible.

## Results and Discussion

The two programs developed for calculating zero-field splitting parameters (one for  $\pi$ -biradicals with  $C_{2v}$  symmetry) are shown in the Appendices, together with a description of the input data and a sample input deck. The programs satisfy numerous criteria for internal consistency. For example, the results vary only slightly with changes in the size and number of the basis-set boxes (Table II). In addition, the predicted D- and E-values are independent of the orientation of the molecules.<sup>19</sup> Finally, the normalization integral (Eq. 3 with  $O=1$ ) approaches 1.0 as the size of the basis orbitals is reduced (Table II).

Unfortunately, there is almost no way to check the two programs externally. The only experimental parameters which can be used for calibration are the ones observed by Closs for the cyclopentadiyl (2).<sup>10</sup> As shown in Table II, these values are significantly lower than the ones calculated using the programs. However the discrepancy may simply be due to an inappropriate geometry.<sup>20</sup> For this reason, a

more extensive series of calculations needs to be performed on the system. It is worth noting that the related systems, 5 and 6, are predicted to have rather similar zero-field splitting parameters (Table II).



5



6

**Table II.** Zero-field splitting parameters calculated using the numerical integration method. The geometries and wavefunctions for the biradicals are explained in Refs. 20 and 21.

Biradical	Basis Orbital Size ( $\text{\AA}/\text{side}$ )	$ D/hc $	$ E/hc $	Normalization
		( $\text{cm}^{-1}$ )	( $\text{cm}^{-1}$ )	Integral
2	[experimental value]	0.084	0.0020	-----
	0.5	0.124	0.0072	0.846
5	0.5	0.122	0.0067	0.858
	0.4	0.122	0.0066	0.932
6	0.5	0.102	0.0020	0.871

## References and Notes

1. For a review of the theoretical and experimental aspects of zero-field splitting parameters, see J.E. Wertz and J.R. Bolton, "'Electron Spin Resonance Elementary Theory and Practical Applications'", McGraw-Hill: New York, 1972.
2. M. Godfrey, C.W. Kern, and M. Karplus, J. Chem. Phys., **44**, 4459 (1966).
3. J.H. van der Waals and G. ter Maten, Mol. Phys., **8**, 301 (1964).
4. A.G. Motten, E.R. Davidson, and A.L. Kwiram, J. Chem. Phys., **75**, 2603 (1981); D. Feller, W.T. Borden, and E.R. Davidson, J. Chem. Phys., **74**, 2256 (1981), and references cited therein.
5. R. McWeeny, J. Chem. Phys., **34**, 399 (1961).
6. J.A. Berson, R.J. Bushby, J.M. McBride, and M. Tremelling, J. Am. Chem. Soc., **93**, 1544 (1971); M. Tremelling and J.M. McBride, unpublished work.
7. D.A. Dougherty and J.A. Berson, unpublished work.
8. L. Salem and C. Rowland, Angew. Chem. Int. Ed., Engl., **11**, 92 (1972).
9. One notable exception is the work by Dougherty and Berson.<sup>7</sup>
10. S.L. Buchwalter and G.L. Closs, J. Am. Chem. Soc., **101**, 4688 (1979).
11. See Section III.
12. See Section IV.
13. The program used for these calculations was an adaptation

- of the one developed by Dougherty and Berson.<sup>7</sup>
14. Huckel Molecular orbitals appear to be adequate for the treatment of planar delocalized triplets.<sup>7</sup>
  15. This discussion closely follows that of Dougherty.<sup>7</sup>
  16. If there are N boxes along one dimension, the corresponding component of the box-to-box vector can vary from (1-N) to (N-1) -- a total of (2N-1) possibilities. This figure must be raised to the power of three because of the three Cartesian axes.
  17. In practice, the only significant saving is in the calculation of the weighting coefficients, since this operation must be performed  $N^6$  times. In fact, it may be advantageous to generate redundant amplitudes because of savings which can later be realized in the evaluation of the weighting factors.
  18. It can be shown that the off-diagonal elements of D do not have to be calculated for  $\pi$ -biradicals with  $C_{2v}$  symmetry. This is true only if the Cartesian axes are made to coincide with the symmetry axes. See the program in Appendix D.
  19. As currently written the program in Appendix D does require the molecules to be oriented in a particular way. Only in this way can symmetry be used to its full advantage.
  20. The geometry of 2 was optimized, within certain limits, by Schaefer: M.P. Conrad, R.M. Pitzer, and H.F. Schaefer, J. Am. Chem. Soc., 101, 2245 (1979). The orbitals for this system were obtained through a Restricted Hartree-Fock (RHF) calculation which was performed with a valence double-zeta basis set (see Section II).

21. The central angle in **5** was set at  $102^\circ$  to coincide with that in **2**. Similarly the five-membered ring in **6** was fixed at the Schaefer geometry for **2.20**. The geometry of the cyclopropane ring was optimized by MNDO. Both the MNDO and RHF calculations on **6** were carried out by Lisa McElwee-White.

## Appendix A

### Description of Input Data for Zero-field Splitting Programs

#### 1. Title Card

TITLE

FORMAT(A80)

#### 2. Control Parameter

PCCARD

FORMAT(I2)

PCCARD

number of primitive control cards

#### 3. Primitive Control Cards

DO I=1, PCCARD

PCATOM(I), PCS(I), PCP(I)

FORMAT (3I5)

PCATOM(I)

number of atoms with primitive  
control scheme I

PCS(I)

number of s-type primitives centered  
at each atom with primitive control  
scheme I

PCP(I)

number of  $p_x$ -type primitives centered  
at each atom with primitive control  
scheme I (it is assumed that the  
number of  $P_x$ ,  $P_y$  and  $P_z$  functions

are the same)

#### 4. Specifications of Integration Grid

XMIN, XMAX, XSTEP

YMIN, YMAX, YSTEP

ZMIN, ZMAX, ZSTEP

FORMAT (3F10.3)

XMIN, YMIN, ZMIN

the minimum x,y, and z values in the  
integration grid (in Å)

XMAX, YMAX, ZMAX

the maximum x,y, and z values in the  
integration grid (in Å)

XSTEP, YSTEP, ZSTEP

the x,y, and z distances between  
points in the integration grid  
(in Å)

#### 5. Atomic Coordinates

DO I=1, NATOM

ATX(I), ATY(I), ATZ(I)

FORMAT (23X, 3D16.8)

NATOM

total number of atoms (calculated  
internally)

ATX(I)

x coordinate of the I-th atom (in Å)

ATY(I)

y coordinate of the I-th atom (in Å)

ATZ(I)

z coordinate of the I-th atom (in Å)

(Note: the format was chosen to conform with that on an  
MQM:INTGEN.LIS output)

## 6. Primitive List

```
DO I=1, NPRIM
PFUNC(I), PEXP(I), PCOEF(I)
FORMAT (22X, I2, 2F15.7)
```

NPRIM	total number of primitive functions (calculated internally)
PFUNC(I)	basis function corresponding to the I-th primitive
PEXP(I)	exponent of the I-th primitive
PCOEF(I)	coefficient of the I-th primitive

(Note: the format was chosen to conform with that on an  
MQM: INTGEN.LIS output)

## 7. Basis Function Coefficients

```
DO I=1, NBF
ABFCOF(I)
FORMAT(D15.8)
DO I=1, NBF
BBFCOF(I)
FORMAT (D15.8)
```

NBF	number of basis functions (calculated
-----	---------------------------------------

internally)

ABFCOF(I)

coefficient of the I-th basis function  
in orbital A

BBFCOF(I)

coefficient of the I-th basis function  
in orbital B

(Note: A listing of coefficients with the proper format can  
easily be obtained by using the MQMX: TRAN2P5 program)

**Appendix B**

**Sample Input Deck**

CALCULATION OF ZFS FOR TRIMETHYLENE // THETA = 102 DEG									
100	2	3	10	5					
200			4	C					
300					2.5000	C.5000			
400					3.0000	C.5000			
500					3.0000	C.5000			
600									
700									
800									
900									
1000									
1100									
1200									
1300									
1400									
1500									
1600									
1700									
1800									
1900									
2000									
2100									
2200									
2300									
2400									
2500									
2600									
2700									
2800									
2900									
3000									
3100									
3200									
3300									
3400									
3500									
3600									
3700									
3800									
3900									
4000									
4100									
4200									
4300									
4400									
4500									
4600									
4700									
4800									
4900									
5000									
5100									
5200									
5300									
5400									
5500									
5600									
5700									
5800									
5900									
6000									
6100									
6200									
6300									
6400									
6500									

8700	CP	Y	25	0.1146000	1.0000000
8700	CP	Z	26	18.1600000	0.0185390
8800	CP	Z	26	3.9840000	0.1154360
8900	CP	Z	26	1.1430000	0.3861880
9000	CP	Z	26	0.3594000	0.6401140
9100	CP	Z	27	0.1146000	1.0000000
9200	FTI	S	28	19.2405600	0.0328280
9300	FTI	S	28	2.8991520	0.2312083
9400	FTI	S	28	0.6534101	0.8172381
9500	FTI	S	29	0.1775765	1.0000000
9600	FTI	S	30	19.2405600	0.0328280
9700	FTI	S	30	2.8991520	0.2312083
9800	FTI	S	30	0.6534101	0.8172381
9900	FTI	S	31	0.1775765	1.0000000
10000	FTI	S	32	19.2405600	0.0328280
10100	FTI	S	32	2.8991520	0.2312083
10200	FTI	S	32	0.6534101	0.8172381
10300	FTI	S	33	0.1775765	1.0000000
10400	FTI	S	34	19.2405600	0.0328280
10500	FTI	S	34	2.8991520	0.2312083
10600	FTI	S	34	0.6534101	0.8172381
10700	FTI	S	35	0.1775765	1.0000000
10800	FTI	S	36	19.2405600	0.0328280
10900	FTI	S	36	2.8991520	0.2312083
11000	FTI	S	36	0.6534101	0.8172381
11100	FTI	S	37	0.1775765	1.0000000
11200	FTI	S	38	19.2405600	0.0328280
11300	FTI	S	38	2.8991520	0.2312083
11400	FTI	S	38	0.6534101	0.8172381
11500	FTI	S	39	0.1775765	1.0000000
11600	0.00000000+00				
11700	0.00000000+00				
11800	0.00000000+00				
11900	0.536127780+00				
12000	0.311055020+00				
12100	0.00000000+00				
12200	0.00000000+00				
12300	0.00000000+00				
12400	0.00000000+00				
12500	0.00000000+00				
12600	0.00000000+00				
12700	0.00000000+00				
12800	0.536127780+00				
12900	0.311055020+00				
13000	0.00000000+00				
13100	0.00000000+00				
13200	0.00000000+00				
13300	0.00000000+00				
13400	0.00000000+00				
13500	0.00000000+00				
13600	0.00000000+00				
13700	0.00000000+00				
13800	0.00000000+00				
13900	0.00000000+00				
14000	0.00000000+00				
14100	0.00000000+00				
14200	0.00000000+00				
14300	0.00000000+00				
14400	0.00000000+00				
14500	0.00000000+00				
14600	0.00000000+00				
14700	0.00000000+00				
14800	0.00000000+00				
14900	0.00000000+00				
15000	0.00000000+00				
15100	0.00000000+00				
15200	0.00000000+00				
15300	0.00000000+00				
15400	0.00000000+00				
15500	0.00000000+00				
15600	0.00000000+00				
15700	0.00000000+00				
15800	0.504652490+00				
15900	0.302753000+00				
16000	0.00000000+00				
16100	0.00000000+00				
16200	0.00000000+00				
16300	0.00000000+00				
16400	0.00000000+00				
16500	0.00000000+00				
16600	0.00000000+00				
16700	0.504652490+00				
16800	0.302753000+00				
16900	0.00000000+00				
17000	0.00000000+00				

17100	0.00000000+00
17200	0.00000000+00
17300	0.00000000+00
17400	0.00000000+00
17500	0.00000000+00
17600	0.524422030-01
17700	0.110552470+00
17800	0.00000000+00
17900	0.00000000+00
18000	0.00000000+00
18100	0.00000000+00
18200	0.00000000+00
18300	0.00000000+00
18400	0.00000000+00
18500	0.00000000+00
18600	0.00000000+00
18700	0.00000000+00
18800	0.00000000+00
18900	0.00000000+00
19000	0.104498520+00
19100	0.153791630+00
19200	0.104498520+00
19300	0.153791630+00

**Appendix C**

**ZFS2: A Program for Calculating Zero-field Splitting  
Parameters in Systems Without Symmetry**

[illegible]

```
*
* *****
*      CALCULATION OF AMPLITUDE ARRAYS
*      *
C*****
C      TCTDIM=XDIM+YDIM*ZDIM
      NTDIMP=TCTDIM+1
      NLSIZE=2*7TDM-1
      NVSIZE=2*XDIM-1
      NWSIZE=2*YDIM-1
      NSSIZE=NLSIZE+NLNIZE
      NTWTCO=NVSIZE+NSSIZE
      DO 207 IJK=1,TCTDIM
        AAMP(IJK)=C.O
        RAMP(IJK)=C.O
        WTCO(IJK)=C.O
      207   DO 209 LPM=NTDIMP,NTWTCO
        WTCO(LPM)=C.O
      209   DO 300 IA=1,NATOM
        NPPOINT=O
        IF (PCP(NSPCA(IA),EC,C) GC TO 300
C*****
C      << HEAVY ATOM SETUP >> *****
      SFIRST=PZLAST+1
      SLAST=PZLAST+PCS(NSPCA(IA))
      PXFIRST=SLAST+1
      PXLAST=SLAST+PCP(NSPCA(IA))
      PYFIRST=PXLAST+1
      PYLAST=PXLAST+PCP(NSPCA(IA))
      PZFIRST=PYLAST+1
      PZLAST=PYLAST+PCP(NSPCA(IA))
      DO 225 II=SFIRST,SLAST
        PNCRN=FCOFF(ITI)*((HALFPI/PEXP(II))*-0.75
        ANCRN(II)=APECCF(PFUNC(II))*PNCRN
        BNCRN(II)=RPECFF(PFUNC(II))*PNCRN
      225   DO 226 JJ=PYFIRST,PYLAST
        PNCRN=PCOFF(JJ)*(((HALFPI/PEXP(JJ))*1.5)/(4.0*PEXP(JJ))*-0.5
        ANCRN(JJ)=APECCF(PFUNC(JJ))*PNCRN
        BNCRN(JJ)=RPECFF(PFUNC(JJ))*PNCRN
      226   DO 227 KK=PYFIRST,PYLAST
        PNCRN=PCOFF(KK)*(((HALFPI/PEXP(KK))*1.5)/(4.0*PEXP(KK))*-0.5
        ANCRN(KK)=APECCF(PFUNC(KK))*PNCRN
        BNCRN(KK)=RPECFF(PFUNC(KK))*PNCRN
      227   DO 228 LL=PZFIRST,PZLAST
        PNCRN=PCOFF(LL)*(((HALFPI/PEXP(LL))*1.5)/(4.0*PEXP(LL))*-0.5
        ANCRN(LL)=APECCF(PFUNC(LL))*PNCRN
        BNCRN(LL)=RPECFF(PFUNC(LL))*PNCRN
      228 C*****
C      << HEAVY ATOM VECTOR >> *****
      DO 258 I=1,XDIM
        XA=XMIN+XSTEP*(I-1)-ATX(IA)
        YA2=XA*XA
      258   DO 297 J=1,YDIM
        YA=YMIN+YSTEP*(J-1)-ATY(IA)
        XYA2=YA*YA+XA2
      297   DO 296 K=1,ZDIM
        ZA=ZMIN+ZSTEP*(K-1)-ATZ(IA)
        RA2=XYA2+ZA*ZA
        NPPOINT=NPPOINT+1
C*****
C      << HEAVY ATOM CALC >> *****
      DO 230 IS=SFIRST,SLAST
        SSTOP=EXP(-1*PEXP(IS)*RA2)
        AAMP(NPPOINT)=AAMP(NPPOINT)+ANCRN(IS)*SSTOP
        RAMP(NPPOINT)=RAMP(NPPOINT)+BNCRN(IS)*SSTOP
      230   DO 235 IPX=PYFIRST,PYLAST
        YSTOP=XA*FXP(-1*PEXP(IPX)*RA2)
        AAMP(NPPOINT)=AAMP(NPPOINT)+ANCRN(IPX)*YSTOP
        RAMP(NPPOINT)=RAMP(NPPOINT)+BNCRN(IPX)*YSTOP
      235   DO 240 IPY=PYFIRST,PYLAST
        YSTOP=YA*FXP(-1*PEXP(IPY)*RA2)
        AAMP(NPPOINT)=AAMP(NPPOINT)+ANCRN(IPY)*YSTOP
        RAMP(NPPOINT)=RAMP(NPPOINT)+BNCRN(IPY)*YSTOP
      240   DO 245 IPZ=PZFIRST,PZLAST
        ZSTOP=ZA*FXP(-1*PEXP(IPZ)*RA2)
        AAMP(NPPOINT)=AAMP(NPPOINT)+ANCRN(IPZ)*ZSTOP
        RAMP(NPPOINT)=RAMP(NPPOINT)+BNCRN(IPZ)*ZSTOP
      245 CONTINUE
      257 CONTINUE
      258 CONTINUE
```

```

16700 C
16800 C ***** << LIGHT ATOM SETUP >> *****
16900 C
17000 C
17100 C
17200 C
17300 C
17400 C
17500 C
17600 C
17700 C
17800 C
17900 C ***** << LIGHT ATOM VECTOR >> *****
18000 C
18100 C
18200 C
18300 C
18400 C
18500 C
18600 C
18700 C
18800 C
18900 C
19000 C
19100 C
19200 C ***** << LIGHT ATOM CALC >> *****
19300 C
19400 C
19500 C
19600 C
19700 C
19800 C
19900 C
20000 C
20100 C
20200 C
20300 C
20400 C
20500 C
20600 C
20700 C
20800 C
20900 C
21000 C
21100 C *****
21200 C *****
21300 C *****
21400 C
21500 C
21600 C *****
21700 C
21800 C
21900 C *****
22000 C
22100 C
22200 C
22300 C
22400 C
22500 C
22600 C
22700 C
22800 C
22900 C
23000 C
23100 C
23200 C
23300 C
23400 C
23500 C
23600 C
23700 C
23800 C
23900 C
24000 C
24100 C
24200 C
24300 C
24400 C
24500 C
24600 C
24700 C
24800 C
24900 C
25000 C
25100 C

```



```

32300 C
32400 WRITE(27,4709)
32500 WRITE(27,4711)(D(I),I=1,3)
32600 WRITE(27,4720)
32700 WRITE(27,4712)
32800 DO 3110 I=1,3
32900 WRITE(27,4713)(X(I,J),J=1,3)
33000 3110 CONTINUE
33100 WRITE(27,4720)
33200 DO 3120 I=1,3
33300 C(I)=ABS(D(I))
33400 3120 CONTINUE
33500 IF (D(1).LE.D(3)) GO TO 3200
33600 CSAV=D(3)
33700 D(3)=D(1)
33800 D(1)=CSAV
33900 3200 EFIN=0.0
34000 3212 EFIN=D(3)*1.5
34100 EFIN=ABS(D(1))-D(2)*0.5
34200 WRITE(27,4714) EFIN
34300 WRITE(27,4715) EFIN
34350 WRITE(27,4720)
34375 WRITE(27,4777) SCALE
34387 WRITE(27,4778) ABNCRN
34400 4701 FORMAT(20A4)
34500 4706 FORMAT(' D TENSOR ELEMENTS ARE :')
34600 4707 FORMAT(' XX XY YY XZ YZ ZZ')
34700 4708 FORMAT(6F10.6)
34800 4709 FORMAT(' DIAGONALIZED D TENSOR ELEMENTS ARE :')
34900 4711 FORMAT(3F10.6)
35000 4712 FORMAT(' EIGENVECTORS OF D TENSOR :')
35100 4713 FORMAT(3F10.6)
35200 4714 FORMAT(' [0]/HC = ',F10.6)
35300 4721 FORMAT(' ',F10.6)
35400 4722 FORMAT(' ')
35500 4715 FORMAT(' [1]/HC = ',F10.6)
35600 4722 FORMAT(' ')
35700 5100 CALCULATION OF ZERO-FIELD SPLITTING PARAMETERS')
35800 5200 BY NUMERICAL INTEGRATION')
35900 5300 GRID SIZE : ',I5,', X',I5,', X',I5)
35950 4777 FORMAT(' SCALING FACTOR : ',D15.8)
35975 4778 FORMAT(' NORMALIZATION : ',D15.8)
36000 9999 STOP
36100 END
36200
36300 C *****
36400 C SDIAG : THE MATRIX DIAGONALIZATION SUBROUTINE
36500 C *****
36600 C
36700 C
36800 C SUBROUTINE SDIAG(N,A,X,D,E)
36900 C SDIAG DIAGONALIZES A REAL SYMMETRIC MATRIX
37000 C METHOD - HOUSEHOLDER REDUCTION TO TRIDIAGONAL FORM, THEN QR
37100 C ITERATIONS TO DIAGONALIZE
37200 C ARGONNE SUBROUTINE LIBRARY ROUTINE F2555
37300 C MINOR MODIFICATIONS - LGV 1/76
37400 C
37500 C INPUT ARGUMENTS
37600 C N - DIMENSION OF MATRIX
37700 C A(N*(N+1)/2) - MATRIX IN PACKED SYMMETRIC FORM (IF N<0 THEN MATRIX
37800 C IS ASSUMED TO BE ALREADY UNPACKED (N BY N))
37900 C X(N,N) - HOLDS ORDERED EIGENVECTORS ON OUTPUT (BY COLUMNS)
38000 C D(N) - HOLDS EIGENVALUES (SMALLEST FIRST) ON OUTPUT
38100 C E(N) - SCRATCH ARRAY
38200 C
38300 C IMPLICIT REAL*8 (A-H,O-Z)
38400 C REAL*8 EPS,A,D,X,E
38500 C DIMENSION A(4),X(3,3),D(3),E(3)
38600 C DATA EPS / 1.0-16/,ILIMIT /40/
38700 C IF (N.LT.0) GO TO 96
38800 C M = N*(N+1)/2 + 1
38900 C DO 97 K = 1,N
39000 C I = N-K+1
39100 C DO 97 L = 1,I
39200 C J = I-L+1
39300 C M = M - 1
39400 C 97 X(I,J) = A(M)
39500 C GO TO 100
39600 C 96 M = N
39700 C N = -N
39800 C DO 95 I = 1,N
39900 C K = K + N
40000 C DO 95 J = 1,I
40100
40200
40300
40400
40500
40600

```

```

40700 64 Y(I,J) = A(I,J)
40800 C-----HOUSEHOLDER REDUCTION
40900 100 NM1 = N - 1
41000 CC 101 NM = 1, NM1
41100 I = N + 1 - NM
41200 P = I - 2
41300 F = X(I,I - 1)
41400 G = F
41500 S = 0.00
41600 IF (M.LT.1) GOTO 99
41700 CC 102 K = 1,M
41800 102 S = S + X(I,K)*X(I,K)
41900 99 E(I) = S
42000 IF (S.EQ.0.00) GO TO 103
42100 P = M + 1
42200 S = S + F * F
42300 G = DSCR1(S)
42400 IF (F.GE.0.00) G = -G
42500 RH = S - F * G
42600 X(I,I - 1) = F - G
42700 F = 0.00
42800 IF (M.LT.1) GOTO 103
42900 CC 107 J = 1,M
43000 X(J,I) = X(I,J)/ RH
43100 S = 0.00
43200 CC 108 K = 1,J
43300 108 S = S + X(J,K) * X(I,K)
43400 JP1 = J + 1
43500 IF (M.LT.JP1) GOTO 98
43600 CC 109 K = JP1, M
43700 109 S = S + X(K,J) * X(I,K)
43800 98 F(J) = S/RH
43900 107 F = F + S * X(J,I)
44000 84 F = F / (RH + RH)
44100 CC 110 J = 1,M
44200 110 F(J) = E(J) - F * X(I,J)
44300 CC 111 J = 1,M
44400 CC 111 K = 1,J
44500 111 Y(J,K) = X(J,K) - X(I,J) * E(K) - X(I,K) * E(J)
44600 C-----END S NOT EQUAL TO ZERO
44700 103 F(I - 1) = G
44800 101 CONTINUE
44900 C-----END I LOOP
45000 C-----ACCUMULATION OF TRANSFORMATION MATRICES
45100 D(I) = 0.00
45200 E(N) = 0.00
45300 F = 0.00
45400 F = 0.00
45500 CC 200 I = 1,N
45600 M = I - 1
45700 IF (D(I).EQ.0.00) GOTO 201
45800 CC 202 J = 1,M
45900 S = 0.00
46000 CC 203 K = 1,M
46100 203 S = S + X(I,K) * X(K,J)
46200 CC 202 K = 1,M
46300 C-----THE FOLLOWING NONSENSE STATEMENT IS NEEDED TO COMBAT COMPILER BUG
46400 L = K + I - K
46500 202 X(K,J) = X(K,J) - S * X(K,L)
46600 C-----END J LOOP
46700 201 E(I) = X(I,I)
46800 X(I,I) = 1.000
46900 IF (M.LT.1) GOTO 200
47000 CC 204 J = 1,M
47100 X(I,J) = 0.00
47200 204 X(J,I) = 0.00
47300 200 CONTINUE
47400 C-----END I
47500 C-----DIAGONALIZATION OF THE TRIDIAGONAL MATRIX
47600 CC 205 L = 1,N
47700 J = 0
47800 RH = EPS * (DABS(D(L)) + DABS(E(L)))
47900 IF (RH.LE.P) GOTO 206
48000 R = RH
48100 C-----TEST FOR SPLITTING
48200 206 CC 207 MP = L,N
48300 P = MP
48400 IF (DABS(F(M)) .LT. R) GOTO 208
48500 207 CONTINUE
48600 C-----LABEL 208 IS TEST FOR CONVERGENCE
48700 208 IF (M.EC.1) GOTO 209
48800 C-----LABEL 209 IS CONVERGENCE
48900 C-----LABEL 210 IS SHIFT
49000 210 P = .500 * (D(L+1) + D(L))
49100 P = DSCR1(P * P + F(L) * E(L))

```

```

49200      RH = D(L) + P - P
49300      IF (P.LT. 0.00) RH=RH+P+P
49400      GO 213 I = L,N
49500      213 C(I) = D(I) - RH
49600      F = F + RH
49700      C-----CR TRANSFORMATION
49800      J = J + 1
49900      P = F(K)
50000      C = 1.000
50100      S = 0.00
50200      MPL = M - L
50300      GO 214 II = 1,MML
50400      I = M - II
50500      R = DSCR1 (P*P + E(I) * E(II))
50600      G = C * E(II)
50700      RH = C * P
50800      F(I+1) = S+R
50900      C = P/R
51000      S = E(II)/ R
51100      C(I+1) = RH + S * (C * G + S * D(II))
51200      GO 214 K = 1,N
51300      RH = X(K,I+1)
51400      P = C * D(II) - S*G
51500      X(K,I+1) = X(K,I) * S + RH * C
51600      214 X(K,I) = X(K,I) * C - RH * S
51700      C-----END K LOOP AND END I LOOP
51800      215 F(L) = S * P
51900      C(L) = C * P
52000      IF (DABS(E(L)).LT. 0) GOTO 209
52100      IF (J.LT. ILIMIT) GOTO 210
52200      COTO 1000
52300      C-----1000 IS ERROR RETURN INDICATING FAILURE OF QR TO CONVERGE
52400      209 C(L) = D(L)+ F
52500      205 CONTINUE
52600      C-----END L LOOP
52700      C-----ORDERING OF EIGENVALUES
52800      GO 300 I = 1,N
52900      K = I
53000      P = D(I)
53100      IP1 = I + 1
53200      IF (N.LT. IP1) GOTO 301
53300      GO 302 J = IP1, N
53400      IF (D(J) .GE. P) GOTO 302
53500      K = J
53600      P = D(J)
53700      302 CONTINUE
53800      C-----END J LOOP
53900      301 IF (K.EQ.I) GOTO 300
54000      C(K) = D(I)
54100      C(I) = P
54200      GO 304 J = 1,N
54300      P = X(J,I)
54400      X(J,I) = X(J,K)
54500      304 X(J,K) = P
54600      300 CONTINUE
54700      C-----END J,END K NOT EQUAL I, I, SDIAG
54800      RETURN
54900      1000 WRITE (6,1002)
55000      1002 FORMAT (// ' ***** UNABLE TO DIAGONALIZE MATRIX ***** ')
55100      STOP 0
55200      END

```

**Appendix D**

**ZFS3: A Program for Calculating Zero-field Splitting  
Parameters in Systems With  $C_{2v}$  Symmetry**

[illegible]

```

120      READ (22,PC5) PFUNC(I),PEXP(I),PCOFF(I)
      NPFC=PFUNC(I)
C
C CCCCCC READ IN BASIS FUNCTION COEFFICIENTS
C
      DO 130 I=1,NPF
      READ (22,PC5) ABFCOF(I)
      DO 135 I=1,NRF
      READ (22,BC5) PRFCOF(I)
      PZLAST=0
C
C *****
C *
C *
C *****
C *****
C
      TOTDIM=XDIM*YDIM*ZDIM
      NYDIMP=TCYDIM+1
      NLSIZE=2*ZDIM-1
      NVSIZE=2*XDIM-1
      NWSIZE=2*YDIM-1
      NSSIZE=NWSIZE*NLSIZE
      NWTCD=NVSIZE*NSSIZE
      DO 207 IJK=1,TCYDIM
      AAMP(IJK)=C.0
      BAMP(IJK)=C.0
      WTCO(IJK)=C.0
      DO 399 IA=1,NATOM
      NPPOINT=0
      IF (PCP(NSPCA(IA)).EQ.0) GO TO 300
C
C *****
C ***** << HEAVY ATOM SETUP >> *****
C
      SFIRST=PZLAST+1
      SLAST=PZLAST+PCS(NSPCA(IA))
      PXFIRST=SLAST+1
      PXLAST=SLAST+PCP(NSPCA(IA))
      PYFIRST=PXLAST+1
      PYLAST=PXLAST+PCP(NSPCA(IA))
      PZFIRST=PYLAST+1
      PZLAST=PYLAST+PCP(NSPCA(IA))
      DO 225 II=SFIRST,SLAST
      PNCRP=PCOFF(II)*((HALFPI/PEXP(II)))**0.75
      ANCRM(II)=ABFCOF(PFUNC(II))*PNCRM
      PNCRM(II)=BFCCOF(PFUNC(II))*PNORM
      DO 226 JJ=PYFIRST,PYLAST
      PNCRP=PCOFF(JJ)*((HALFPI/PEXP(JJ)))**1.5/((4.0*PEXP(JJ)))**0.5
      ANCRM(JJ)=ABFCOF(PFUNC(JJ))*PNCRM
      PNCRM(JJ)=BFCCOF(PFUNC(JJ))*PNCRM
      DO 227 KK=PYFIRST,PYLAST
      PNCRP=PCOFF(KK)*((HALFPI/PEXP(KK)))**1.5/((4.0*PEXP(KK)))**0.5
      ANCRM(KK)=ABFCOF(PFUNC(KK))*PNCRM
      PNCRM(KK)=BFCCOF(PFUNC(KK))*PNORM
      DO 228 LL=PZFIRST,PZLAST
      PNCRP=PCOFF(LL)*((HALFPI/PEXP(LL)))**1.5/((4.0*PEXP(LL)))**0.5
      ANCRM(LL)=ABFCOF(PFUNC(LL))*PNCRM
      BNCRM(LL)=BFCCOF(PFUNC(LL))*PNCRM
C
C *****
C ***** << HEAVY ATOM VECTOR >> *****
C
      DO 229 I=1,XDIM
      XA=XPIN+XSTEP*(I-1)-ATX(IA)
      YA2=XA*XA
      DO 297 J=1,YDIM
      YA=YPIN+YSTEP*(J-1)-ATY(IA)
      XYA2=YA*YA+YA2
      DO 296 K=1,ZDIM
      ZA=ZPIN+ZSTEP*(K-1)-ATZ(IA)
      RA2=XYA2+ZA*ZA
      NPPOINT=NPPOINT+1
C
C *****
C ***** << HEAVY ATOM CALC >> *****
C
      DO 230 IS=SFIRST,SLAST
      SSTORE=EXP(-1*PEXP(IS)*RA2)
      AAMP(NPPOINT)=AAMP(NPPOINT)+ANCRM(IS)*SSTORE
      BAMP(NPPOINT)=BAMP(NPPOINT)+BNCRM(IS)*SSTORE
      DO 235 IPX=PXFIRST,PXLAST
      XSTORE=XA*EXP(-1*PEXP(IPX)*RA2)
      AAMP(NPPOINT)=AAMP(NPPOINT)+ANCRM(IPX)*XSTORE
      BAMP(NPPOINT)=BAMP(NPPOINT)+BNCRM(IPX)*XSTORE
      DO 240 IPY=PYFIRST,PYLAST
      YSTORE=YA*EXP(-1*PEXP(IPY)*RA2)
      AAMP(NPPOINT)=AAMP(NPPOINT)+ANCRM(IPY)*YSTORE
      BAMP(NPPOINT)=BAMP(NPPOINT)+BNCRM(IPY)*YSTORE

```

```

17000 240 RAMP(NPOINT)=RAMP(NPOINT)+PNCRM(IPY)*YSTOP
17100 IF 245 IP7=P7FIPST,P7LAST
17200 ZSTOP=ZA*FYP(-1)*PEXP(IP7)*PA2)
17300 AAMP(NPOINT)=AAMP(NPOINT)+ANCRM(IP7)*ZSTOP
17400 245 RAMP(NPOINT)=RAMP(NPOINT)+PNCRM(IP7)*ZSTOP
17500 246 CONTINUE
17600 247 CONTINUE
17700 248 CONTINUE
17800 GO TC 399
17900
18000 C
18100 C+**** ***** << LIGHT ATOM SETUP >> *****
18200 C
18300 300 SFIRST=PZLAST+1
18400 SLAST=PZLAST+PCS(NSPCA(IA))
18500 PZLAST=SLAST
18600 DO 305 NN=SFIRST,SLAST
18700 PNCRM=PCCEF(NN)*(HALFP)/PEXP(NN)**-0.75
18800 ANCRM(NN)=ARFCCF(PFUNC(NN))*PNORM
18900 BNCRM(NN)=RBFCCF(PFUNC(NN))*PNCRM
19000 305
19100 C
19200 C+**** ***** << LIGHT ATOM VECTOR >> *****
19300 C
19400 DO 316 I=1,XDIM
19500 XA=XPIA+XSTEP*(I-1)-ATX(IA)
19600 YA2=YA*XA
19700 DO 317 J=1,YDIM
19800 YA=YPIA+YSTEP*(J-1)-ATY(IA)
19900 XYA2=YA*YA+YA2
20000 DO 316 K=1,ZDIM
20100 ZA=ZPIA+ZSTEP*(K-1)-ATZ(IA)
20200 RA2=XYA2+ZA*ZA
20300 NPOINT=NPOINT+1
20400 C
20500 C+**** ***** << LIGHT ATOM CALC >> *****
20600 C
20700 DO 310 IS=SFIRST,SLAST
20800 SSTOP=FXF(-1)*PEXP(IS)*RA2)
20900 AAMP(NPOINT)=AAMP(NPOINT)+ANCRM(IS)*XSTOP
21000 BAMP(NPOINT)=BAMP(NPOINT)+BNCRM(IS)*XSTOP
21100 310 CONTINUE
21200 316 CONTINUE
21300 317 CONTINUE
21400 318 CONTINUE
21500 319 CONTINUE
21600 FC1 FORMAT (3I5)
21700 FC2 FORMAT (3F10.3)
21800 FC3 FORMAT (23X,3D16.8)
21900 FC4 FORMAT (22X,I2,2F15.7)
22000 FC5 FORMAT (D15.8)
22100 FC6 FORMAT (ARC)
22200 FC7 FORMAT (I2)
22300 C
22400 C+**** *****
22500 C+**** *****
22600 C+**** *****
22700 C+**** *****
22800 C+**** *****
22900 C+**** *****
23000 C+**** *****
23100 C
23200 ISHSZ=YDIM*ZDIM
23300 C
23400 C+**** ***** << INCREMENT ELECTRON I OVER QUADRANT 1 >> *****
23500 C
23600 DO 1600 IX=1,XSTOP
23700 ISTRX=XSTOP-IX
23800 CZFC1=ISTRX.FC.C
23900 INDY1=(IX-1)*ISHSZ
24000 DO 1500 IY=1,YSTOP
24100 ISTRY=YSTOP-IY
24200 CZFC2=ISTRY.FC.C
24300 INDY2=INDY1+(IY-1)*ZDIM
24400 DO 1400 IZ=1,ZSTOP
24500 JPOINT=0
24600 IPOINT=INDY2+IZ
24700 AAMPI=AAMP(IPOINT)
24800 BAMPI=BAMP(IPOINT)
24900 AXBI=AAMPI*BAMPI
25000 AAPPI2=AAMPI*AAMPI
25100 BAMP12=BAMPI*BAMPI
25200 C
25300 C+**** ***** << INCREMENT ELECTRON J OVER QUADRANT 1 >> *****
25400 C

```

```

24200 DD 1200 JY=1,YSTOP
24300 FACTR1=1.0
24400 JSTRY=JY-YSTOP
24500 IF (C7ECH1.AND.(JSTRY.EQ.0)) FACTR1=C.5
24600 IN1=ARS(JX-IX)*ISM57+1
24700 DD 1170 JY=1,YSTOP
24800 FACTR2=1.0
24900 JSTRY=JY-YSTOP
25000 IF (C7ECH2.AND.(JSTRY.EQ.0)) FACTR2=C.5
25100 FAX=FACTR1*FACTR2
25200 IN2=IN1+ARS(JY-1Y)*ZDIM
25300 DD 1160 JZ=1,ZDIM
25400 INDEX=IN2+ARS(JZ-1Z)
25500 JPCINT=JPCINT+1
25600 AAMPJ=AAMP(JPCINT)
25700 RAMPJ=RAMP(JPCINT)
25800 WTCO(INDEX)=WTCO(INDEX)+(AAMPJ+RAMPJ-AXBI+RAMPJ+AAMPJ)*FAX
25900
26000 1160 CONTINUE
26100 1170 CONTINUE
26200
26300 C
26400 C+++++ << INCREMENT ELECTRON J OVER QUADRANT 2>> ++++++
26500 C
26600 DD 1190 JY=YSTEP1,YDIM
26700 FACTR2=1.0
26800 JSTRY=JY-YSTOP
26900 IF (C7ECH2.AND.(JSTRY.EQ.0)) FACTR2=C.5
27000 FAX=FACTR1*FACTR2
27100 IN2=IN1+ARS(JY-1Y)*ZDIM
27200 DD 1180 JZ=1,ZDIM
27300 INDEX=IN2+ARS(JZ-1Z)
27400 JPCINT=JPCINT+1
27500 AAMPJ=AAMP(JPCINT)
27600 RAMPJ=RAMP(JPCINT)
27700 COC=AAMPJ+RAMPJ+RAMPJ
27800 WTCO(INDEX)=WTCO(INDEX)+(COC-AXBI+RAMPJ+AAMPJ)*FAX
27900
28000 1180 CONTINUE
28100 1190 CONTINUE
28200 1200 CONTINUE
28300
28400 C
28500 C+++++ << INCREMENT ELECTRON J OVER QUADRANTS 3 AND 4 >> ++++++
28600 C
28700 DD 1300 JX=XSTEP1,XDIM
28800 FACTR1=1.0
28900 JSTRX=JX-XSTOP
29000 IF (C7ECH1.AND.(JSTRX.EQ.0)) FACTR1=C.5
29100 IN1=ARS(JX-IX)*ISM57+1
29200 DD 1290 JY=1,YDIM
29300 FACTR2=1.0
29400 JSTRY=JY-YSTOP
29500 IF (C7ECH2.AND.(JSTRY.EQ.0)) FACTR2=C.5
29600 FAX=FACTR1*FACTR2
29700 IN2=IN1+ARS(JY-1Y)*ZDIM
29800 DD 1280 JZ=1,ZDIM
29900 INDEX=IN2+ARS(JZ-1Z)
30000 JPCINT=JPCINT+1
30100 AAMPJ=AAMP(JPCINT)
30200 RAMPJ=RAMP(JPCINT)
30300 COC=AAMPJ+RAMPJ+RAMPJ
30400 WTCO(INDEX)=WTCO(INDEX)+(COC-AXBI+RAMPJ+AAMPJ)*FAX
30500
30600 1280 CONTINUE
30700 1290 CONTINUE
30800 1300 CONTINUE
30900 1400 CONTINUE
31000 1500 CONTINUE
31100 1600 CONTINUE
31200
31300 C
31400 C+++++
31500 C+++++
31600 C+++++
31700 C
31800 C
31900 C
32000 C
32100 C
32200 C
32300 C
32400 C
32500 C
32600 C
32700 C
32800 C
32900 C
33000 C
33100 C
33200 C
33300 C
33400 C
33500 C
33600 C
33700 C
33800 C
33900 C
34000 C
34100 C
34200 C
34300 C
34400 C
34500 C
34600 C
34700 C
34800 C
34900 C
35000 C
35100 C
35200 C
35300 C
35400 C
35500 C
35600 C
35700 C
35800 C
35900 C
36000 C
36100 C
36200 C
36300 C
36400 C
36500 C
36600 C
36700 C
36800 C
36900 C
37000 C
37100 C
37200 C
37300 C
37400 C
37500 C
37600 C
37700 C
37800 C
37900 C
38000 C
38100 C
38200 C
38300 C
38400 C
38500 C
38600 C
38700 C
38800 C
38900 C
39000 C
39100 C
39200 C
39300 C
39400 C
39500 C
39600 C
39700 C
39800 C
39900 C
40000 C
40100 C
40200 C
40300 C
40400 C
40500 C
40600 C
40700 C
40800 C
40900 C
41000 C
41100 C
41200 C
41300 C
41400 C
41500 C
41600 C
41700 C
41800 C
41900 C
42000 C
42100 C
42200 C
42300 C
42400 C
42500 C
42600 C
42700 C
42800 C
42900 C
43000 C
43100 C
43200 C
43300 C
43400 C
43500 C
43600 C
43700 C
43800 C
43900 C
44000 C
44100 C
44200 C
44300 C
44400 C
44500 C
44600 C
44700 C
44800 C
44900 C
45000 C
45100 C
45200 C
45300 C
45400 C
45500 C
45600 C
45700 C
45800 C
45900 C
46000 C
46100 C
46200 C
46300 C
46400 C
46500 C
46600 C
46700 C
46800 C
46900 C
47000 C
47100 C
47200 C
47300 C
47400 C
47500 C
47600 C
47700 C
47800 C
47900 C
48000 C
48100 C
48200 C
48300 C
48400 C
48500 C
48600 C
48700 C
48800 C
48900 C
49000 C
49100 C
49200 C
49300 C
49400 C
49500 C
49600 C
49700 C
49800 C
49900 C
50000 C
50100 C
50200 C
50300 C
50400 C
50500 C
50600 C
50700 C
50800 C
50900 C
51000 C
51100 C
51200 C
51300 C
51400 C
51500 C
51600 C
51700 C
51800 C
51900 C
52000 C
52100 C
52200 C
52300 C
52400 C
52500 C
52600 C
52700 C
52800 C
52900 C
53000 C
53100 C
53200 C
53300 C
53400 C
53500 C
53600 C
53700 C
53800 C
53900 C
54000 C
54100 C
54200 C
54300 C
54400 C
54500 C
54600 C
54700 C
54800 C
54900 C
55000 C
55100 C
55200 C
55300 C
55400 C
55500 C
55600 C
55700 C
55800 C
55900 C
56000 C
56100 C
56200 C
56300 C
56400 C
56500 C
56600 C
56700 C
56800 C
56900 C
57000 C
57100 C
57200 C
57300 C
57400 C
57500 C
57600 C
57700 C
57800 C
57900 C
58000 C
58100 C
58200 C
58300 C
58400 C
58500 C
58600 C
58700 C
58800 C
58900 C
59000 C
59100 C
59200 C
59300 C
59400 C
59500 C
59600 C
59700 C
59800 C
59900 C
60000 C
60100 C
60200 C
60300 C
60400 C
60500 C
60600 C
60700 C
60800 C
60900 C
61000 C
61100 C
61200 C
61300 C
61400 C
61500 C
61600 C
61700 C
61800 C
61900 C
62000 C
62100 C
62200 C
62300 C
62400 C
62500 C
62600 C
62700 C
62800 C
62900 C
63000 C
63100 C
63200 C
63300 C
63400 C
63500 C
63600 C
63700 C
63800 C
63900 C
64000 C
64100 C
64200 C
64300 C
64400 C
64500 C
64600 C
64700 C
64800 C
64900 C
65000 C
65100 C
65200 C
65300 C
65400 C
65500 C
65600 C
65700 C
65800 C
65900 C
66000 C
66100 C
66200 C
66300 C
66400 C
66500 C
66600 C
66700 C
66800 C
66900 C
67000 C
67100 C
67200 C
67300 C
67400 C
67500 C
67600 C
67700 C
67800 C
67900 C
68000 C
68100 C
68200 C
68300 C
68400 C
68500 C
68600 C
68700 C
68800 C
68900 C
69000 C
69100 C
69200 C
69300 C
69400 C
69500 C
69600 C
69700 C
69800 C
69900 C
70000 C
70100 C
70200 C
70300 C
70400 C
70500 C
70600 C
70700 C
70800 C
70900 C
71000 C
71100 C
71200 C
71300 C
71400 C
71500 C
71600 C
71700 C
71800 C
71900 C
72000 C
72100 C
72200 C
72300 C
72400 C
72500 C
72600 C
72700 C
72
```

```

23500 2000 A(1)=0.0
23500 DO 2500 I=1,XDIM
23500 IDY=I-1
23500 ICXX=ICX+ICX
23500 FDXX=ICX+XXINC
23500 FDXX3=FDXX+3.0
23500 DO 2400 J=1,YDIM
23500 IDY=J-1
23500 IDYY=IDY+IDY
23500 FDYY=IDY+YYINC
23500 FDYY3=FDYY+3.0
23500 ICXXYY=ICXX+IDYY
23500 FDXXYY=FDXX+FDYY
23500 DO 2300 K=1,ZDIM
23500 INDEX=INDEX+1
23500 IDZ=K-1
23500 IDZZ=IDZ+IDZ
23500 IDPP=IDXXYY+IDZZ
23500 GWTCC=WTCC(INDEX)
23500 SCALE=SCALE+GWTCC
23500 IF (IDRR.EQ.0) GO TO 2300
23500 FDZZ=IDZZ+ZZINC
23500 DIST2=FDXXYY+FDZZ
23500 DIST5=DIST2**2.5
23500 A(1)=A(1)+GWTCC*(DIST2-FDXX3)/DIST5
23500 A(2)=A(2)+GWTCC*(DIST2-FDYY3)/DIST5
23500 A(3)=A(3)+GWTCC*(DIST2-3.0*FDZZ)/DIST5
23500 2300 CONTINUE
23500 2400 CONTINUE
23500 2500 CONTINUE
23500 DO 3000 I=1,3
23500 A(I)=A(I)+5.8571593/SCALE
23500 A(I)=ABS(A(I))
23500 3000 CONTINUE
23500 ABNORM=SCALE*XYZINC*XYZINC*4.0
23500 C
23500 C***** ORDERING OF D-TENSOR ELEMENTS
23500 C
23500 D(3)=MAX(A(1),A(2),A(3))
23500 D(1)=MIN(A(1),A(2),A(3))
23500 IF (A(1).EQ.D(3)) GO TO 3840
23500 IF (A(1).EQ.D(1)) GO TO 3820
23500 D(2)=A(1)
23500 GO TO 3850
23500 3820 IF (A(2).EQ.D(3)) GO TO 3830
23500 D(2)=A(2)
23500 GO TO 3850
23500 3830 D(2)=A(3)
23500 GO TO 3850
23500 3840 IF (A(2).EQ.D(1)) GO TO 3850
23500 D(2)=A(2)
23500 GO TO 3850
23500 3850 D(2)=A(3)
23500 C
23500 C***** FINAL OUTPUT
23500 C
23500 3890 WRITE (27,4820)
23500 WRITE (27,5100)
23500 WRITE (27,5200)
23500 WRITE (27,4820)
23500 WRITE (27,510) TITLE
23500 WRITE (27,4820)
23500 WRITE (27,4820)
23500 WRITE (27,5300) XDIM,YDIM,ZDIM
23500 WRITE (27,4820)
23500 WRITE (27,4709)
23500 WRITE (27,4711) (D(I),I=1,3)
23500 WRITE (27,4820)
23500 3200 EFIN=0.0
23500 3212 DFIN=D(3)+1.5
23500 EFIN=ABS(D(1)-D(2))*C.5
23500 WRITE (27,4714) DFIN
23500 WRITE (27,4715) EFIN
23500 WRITE (27,4820)
23500 WRITE (27,4877) SCALE
23500 WRITE (27,4878) ABNORM
23500 4701 FORMAT(2CA4)
23500 4702 FORMAT(6F10.6)
23500 4703 FORMAT(' DIAGONALIZED D TENSOR ELEMENTS ARE :')
23500 4711 FORMAT(3F10.6)
23500 4712 FORMAT(3F10.6)
23500 4714 FORMAT(' [I]/HC = ',F10.6)
23500 4715 FORMAT(' ',F10.6)
23500 4716 FORMAT(' ')
23500 4717 FORMAT(' [E]/HC = ',F10.6)

```

```

41500      4720      FORMAT(' ')
41600      5100      FORMAT('          CALCULATION OF ZERO-FIELD SPLITTING PARAMETERS')
41700      5200      FORMAT('          BY NUMERICAL INTEGRATION')
41800      5300      FORMAT(' GRID SIZE : ',I5,' X ',I5,' X ',I5)
41850      4877      FORMAT(' SCALING FACTOR : ',D15.8)
41875      4878      FORMAT(' NORMALIZATION : ',D15.8)
41900      0999      STOP
42000      END

```